Journal Pre-proof

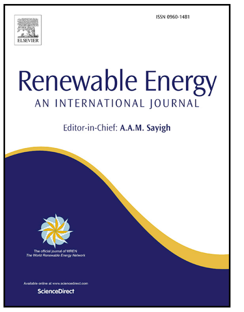

A Thermal Power Budget Approach to Evaluate the Geothermal Potential of a Flooded Open-Pit Mine: Case Studies from the Carey Canadian and King-Beaver Mines (Canada)

Samuel Lacombe, Félix-Antoine Comeau, Jasmin Raymond

PII: S0960-1481(24)02392-9

DOI: https://doi.org/10.1016/j.renene.2024.122324

Reference: RENE 122324

To appear in: *Renewable Energy*

Received Date: 16 April 2024

Revised Date: 7 December 2024

Accepted Date: 29 December 2024

A Thermal Power Budget Approach to Evaluate the Geothermal Potential of a Flooded Open-Pit Mine: Case Studies from the Carey Canadian and King-Beaver Mines (Canada)

Samuel Lacombe
Institut national de la recherche scientifique
Centre Eau Terre Environnement
490, rue de la Couronne, Québec (Québec) G1K 9A9
samuel.lacombe@inrs.ca
*First author

Félix-Antoine Comeau
Institut national de la recherche scientifique
Centre Eau Terre Environnement
490, rue de la Couronne, Québec (Québec) G1K 9A9
felix-antoine.comeau@inrs.ca
*Corresponding author

Jasmin Raymond
Institut national de la recherche scientifique
Centre Eau Terre Environnement
490, rue de la Couronne, Québec (Québec) G1K 9A9
jasmin.raymond@inrs.ca

A Thermal Power Budget Approach to Evaluate the Geothermal Potential of a Flooded Open-Pit Mine: Case Studies from the Carey Canadian and King-Beaver Mines (Canada)

ABSTRACT

Following mine closure, open-pit mines gradually fill with ground and surface water. Due to its thermal inertia, this water maintains a relatively stable temperature year round, making it suitable for heating and cooling buildings. Previous estimates of the geothermal potential of a flooded open-pit mine primarily focused on the water volume alone, often underestimating the total potential by neglecting heat exchanges with the surrounding rock and incoming water. This paper introduces a novel analytical approach based on an improve thermal power balance concept to better estimate the geothermal potential of a flooded open-pit mine. Over a 25-years analysis, it was shown that the host rock can contribute over 15 % of the thermal energy in the water, while water supply can double this energy. The method developed is both quick and reliable, allowing for early stage evaluation of geothermal resources by accounting not only for the mine's water volume but also energy inputs from precipitation, runoff, groundwater recharge and the host rock. The study focuses on the Carey Canadian and King-Beaver open-pits, two closed asbestos mines in southern Quebec (Canada).

KEYWORDS

Mine water; Cooling; Heat pump; Open-loop; Rock thermal property; Pit lake

ABBREVIATIONS

Abbreviations
BBL : Baie Verte-Brompton Line
COP : Coefficient Of Performance
DEM : Digital Elevation Models
DTM : Digital Terrain Model
GHP : Geothermal Heat Pump
SAL : Société Asbestos Limitée
TCS : Thermal Conductivity Scanner
USA : United States of America
USGS : United States Geological Survey

Measurement units
°C : Degree Celsius
J : Joule
MJ : Megajoule
K : Kelvin
m : Meter
km : Kilometre
mm : Millimetre
s : Second
W : Watt
MW : Megawatt
yr :Year

Symbols and Greek letters
σ : Median (-)
∞ : Infinity (-)
± : More or less (-)
Δ : Difference (-)
a : Thermal diffusivity (m^2s^{-1})

Variables
c : Volumetric heat capacity ($Jm^{-3}K^{-1}$)
C_p : Runoff coefficient (-)
D : Deficit soil moisture ($mmyr^{-1}$)
E : Thermal Energy (J)
F : Correction coefficient (-)
G : Recharge ($mmyr^{-1}$)
i : Monthly thermal index (-)
I : Infiltration capacity ($mmyr^{-1}$)
I_t : Annual thermal index (-)
Int : Contour line interval (m)
L : Length of grid lines (m)
n : Number of bands (-)
N : Number of grid lines (-)
P : Precipitation rate ($mmyr^{-1}$)
PET : Potential evapotranspiration ($mmyr^{-1}$)
Q : Thermal power (W)
Q_b : Thermal power for building (W)
R : Runoff ($mmyr^{-1}$)
RET : Real evapotranspiration ($mmyr^{-1}$)
S : Water reserve at the soil surface ($mmyr^{-1}$)
S_b : Average watershed slope (%)
t : Time (s)
T : Temperature (°C or K)
T_g : Undisturbed ground temperature (°C or K)
V : Volume (m^3)
x : Horizontal component (m)
y : Horizontal component (m)
z : Vertical component (m)

Indexes
amb : Ambient air
d : Dynamic
G : Groundwater
f : Final
h : Vertical
init : Initial
max : Maximal
P : Precipitation
r : Rock
R : Runoff
s : Static
tot : Total
v : Horizontal
w : Water

1. INTRODUCTION

Although mining sites require significant investments to enable their exploitation, they have historically been considered to hold very little value after closure. The reasons for their abandonment often revolve around the depletion of mineral resources, non-compliance with mining safety requirements, or political decisions [1], as well as the absence of mine reclamation plans and post-mining management by legislative authorities [2]. However, the situation is beginning to change, and there is now increasing interest in their reuse, such as tourist and cultural attractions, waste storage or water reservoirs for local communities. Another topic gaining increasing attention is the production of renewable geothermal energy [3,4,5].

Geothermal resources stand out among recognized renewable energy sources like wind, hydroelectricity and solar power for their ability to reduce greenhouse gas emissions [6,7,8]. Geothermal heat pumps (GHPs) are increasingly used to heat and cool buildings due to their efficiency and adaptability to various geological environments [9,10]. After closure, underground tunnel networks and open-pits become flooded with groundwater and runoff. This volume of water, maintained at a constant temperature throughout the year due to the Earth's heat flux, possesses thermal energy that can be utilized through GHPs to meet the heating and cooling energy needs of industrial and residential areas. Since this groundwater occupies cavities that were excavated during mine operations (open-pit or underground workings), it is accessible without the need for drilling, which is often the primary expense associated with geothermal energy recovery. This technology would be advantageously deployed in areas where municipalities aim to give a second life to dormant mining sites [11,12].

The first GHP system using groundwater from abandoned underground mine workings reported in the literature was installed in 1989 in Springhill (Nova Scotia, Canada; [13]), marking the feasibility and economic viability of this approach. This led to further studies exploring the untapped thermal resource potential in flooded underground mine sites. Presently, the predominant use of low-temperature geothermal resources in mine sites is in flooded underground mines, where high-permeability network enables groundwater pumping and injection at significant depths and flow rates to supply GHP systems [14,15,16,17,18,19,20,21]. Compared to underground mines, less attention has been given to the geothermal potential of open-pit mines [15,19].

Though open-pit mines and natural lakes may seem similar, they differ significantly. Natural lakes can't handle unacceptable temperature changes (>1°C) that would significantly damage the lake's ecology, amenity value or value as a resource [22,23], while artificial flooded open pits aren't restricted by this. Natural lakes are shallow (under 10–15 m) and experience seasonal temperature shifts, whereas flooded open pits are deeper (over 100 m) and have stable temperatures year-round. Thus, the methodology developed to define the heat balance of the natural lake [24,25] must be adapted to place less emphasis on surface interactions and more on the surrounding rock.

Nevertheless, notable examples are already highlighting the promise of open-pit resources. For instance, in 2006, a system was installed at the flooded Goyer quarry in Saint-Bruno-de-Montarville (Quebec, Canada), demonstrating the use of its 8,000,000 m^3 water reservoir to provide heating and cooling for a modern condominium complex, resulting in energy savings of 40 to 50 % [7,11]. More recently, a study in Turin (Italy) evaluated the potential of nearly 20 abandoned and flooded quarries, collectively containing over 10,000,000 m^3 of water, for supplying thermal energy to nearby agro-industrial buildings [26]. In Spain, another study aimed to use the water from a lake formed by an abandoned zinc mine, with a volume of approximately 30,000,000 m^3, mainly relying on hydrogeological and hydrochemical characterization to evaluate its geothermal potential [27].

The longstanding mining history in the province of Quebec (Canada) has led to the development of small communities located near mining operations [28]. This has resulted in a landscape marked by mining activities, both underground and on the surface. Several of these operations occurred in the southern part of Quebec, where the population continues to grow around these remains (Figure 1). The sites mainly consist of quarries and open-pit mines, many of which are now partially or entirely flooded. These abandoned sites can now be considered as opportunities for geothermal energy use, promoting the socio-economic acceptability of developing industrial and residential areas in the mining environment and facilitating restoration.

Unlike water body in underground mines, the thermal regime of a flooded open-pit mine is mainly influenced by atmospheric conditions [29,30]. While the extractable thermal energy of pit lakes has traditionally been considered static and assessed only on available volume of water, recent research reveals a more dynamic picture. Pit lakes act as a battery, continuously recharged by atmospheric exchanges (such as solar radiation, evaporation, precipitation, runoff, wind, and variations in ambient air temperature) and interactions with the ground (including terrestrial heat flux, groundwater flow, and the host rock). These exchanges represent dynamic thermal fluxes to the water reservoir containing thermal energy.

Recognizing the limitations of static energy estimation, recent studies advocate for comprehensive heat balance models that incorporate dynamic energy contributions from groundwater and host rock into the assessment of abandoned and flooded underground mines [17,19,31]. However, methods for estimating this resource in pit lakes remain limited. Existing approaches often rely solely on static energy, resulting in underestimation of available thermal energy [26,32]. The current study thus focuses on open-pit mines, and the approach is different for an underground mine where the volume of water is distributed in a cluster of coiled underground tunnels rather than in a single pit. As a result, the contact surface with the rock is greater for an underground compared to an open pit mine and contributes more to the thermal power budget. Ngoyo Mandemvo et al [31] have examined this case of an underground mine and used the finite line source equation to determine the amount of heat that can be extracted from the host rock, which is different from the approach we propose for an open pit mine.

To address this gap, the objective of our research was to introduce a novel analytical approach integrating both static and dynamic thermal energy contributions, enhancing geothermal resource quantification in pit lakes. This approach simplifies thermal processes and system geometry, providing a comprehensive yet straightforward estimation of the energy resource. By supplying critical information for decision-making at early project stages, it facilitates further resource development or infrastructure investments. Understanding geothermal potential not only adds value to abandoned mines but also justifies restoration efforts. Thus, efficient assessment methods for flooded open-pit mine geothermal resources are crucial in early development stages. Illustrative examples of this analytical approach are given for the Carey Canadian and King Beaver flooded pits, owned by Société Asbestos Limitée (SAL) in Thetford Mines, Canada. These sites, chosen for their potential for residential and industrial development, demonstrate the practical application of the proposed methodology (Figure 1).

2. GEOLOGICAL SETTINGS

The King-Beaver (1878-2008) and Carey Canadian (1955-1986) mines both exploited chrysotile asbestos and talc in southern Quebec, where the temperature typically varies from -17 to 23 °C over the course of the year, and heating degree days (18 °C) are about 5000. The deposits are located in the Appalachian geological province, between the Humber and Dunnage tectonostratigraphic zones, delineated by the Baie Verte-Brompton Line (BBL). Ophiolitic sequences, found in diverse forms and sizes, border the BBL in southern Quebec [33,34] (Figure 1).

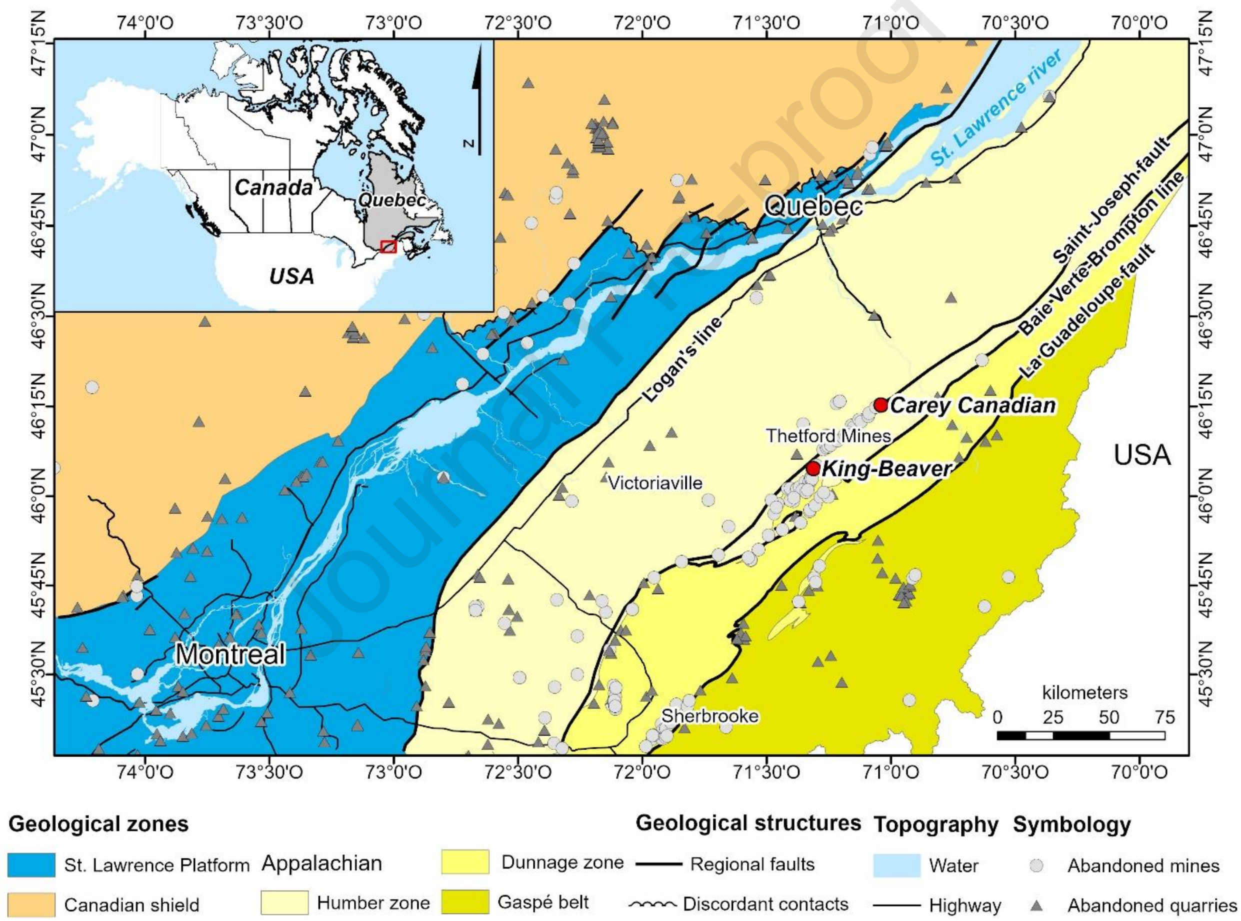

Figure 1. Mining history, location of pilot sites and regional geological context [35,36].

The Carey Canadian open-pit mine is located approximately 30 km northeast of Thetford Mines (Figure 1). This deposit represents the termination of a serpentinized peridotite sheet (Pennington dyke), with a maximum width of approximately 200 m, and stretches for over 50 km in a northeasterly direction from Thetford Mines [33]. The dyke's inclination varies in alignment with the schists and surrounding metasedimentary rocks, and constitutes the southeastern flank of a significant anticline [37] (Figure 2).

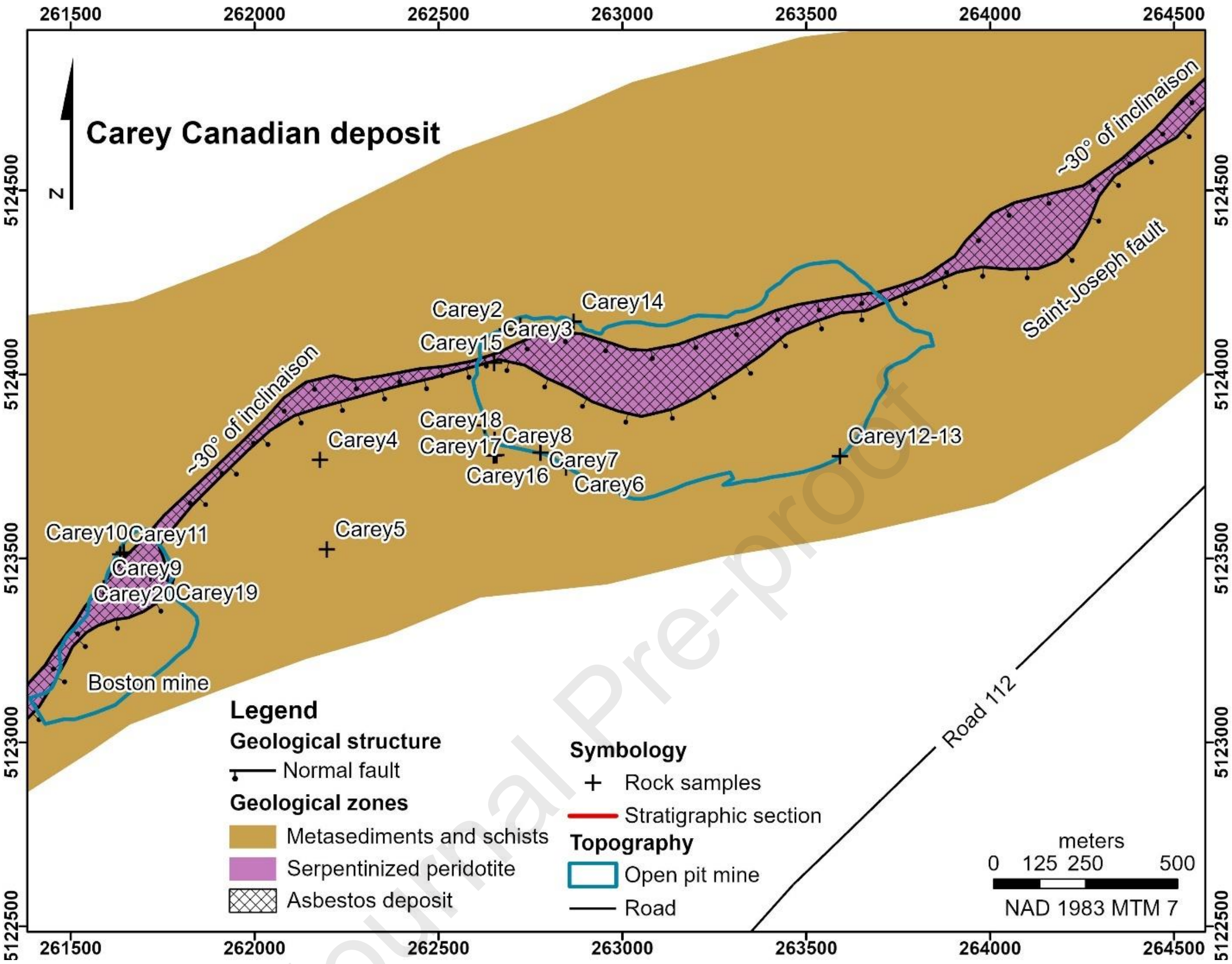

Figure 2. Bedrock geology map of the Carey Canadian mine with locations of rock samples (adapted from Riordon [37]). The location of the mine is shown in Figure 1.

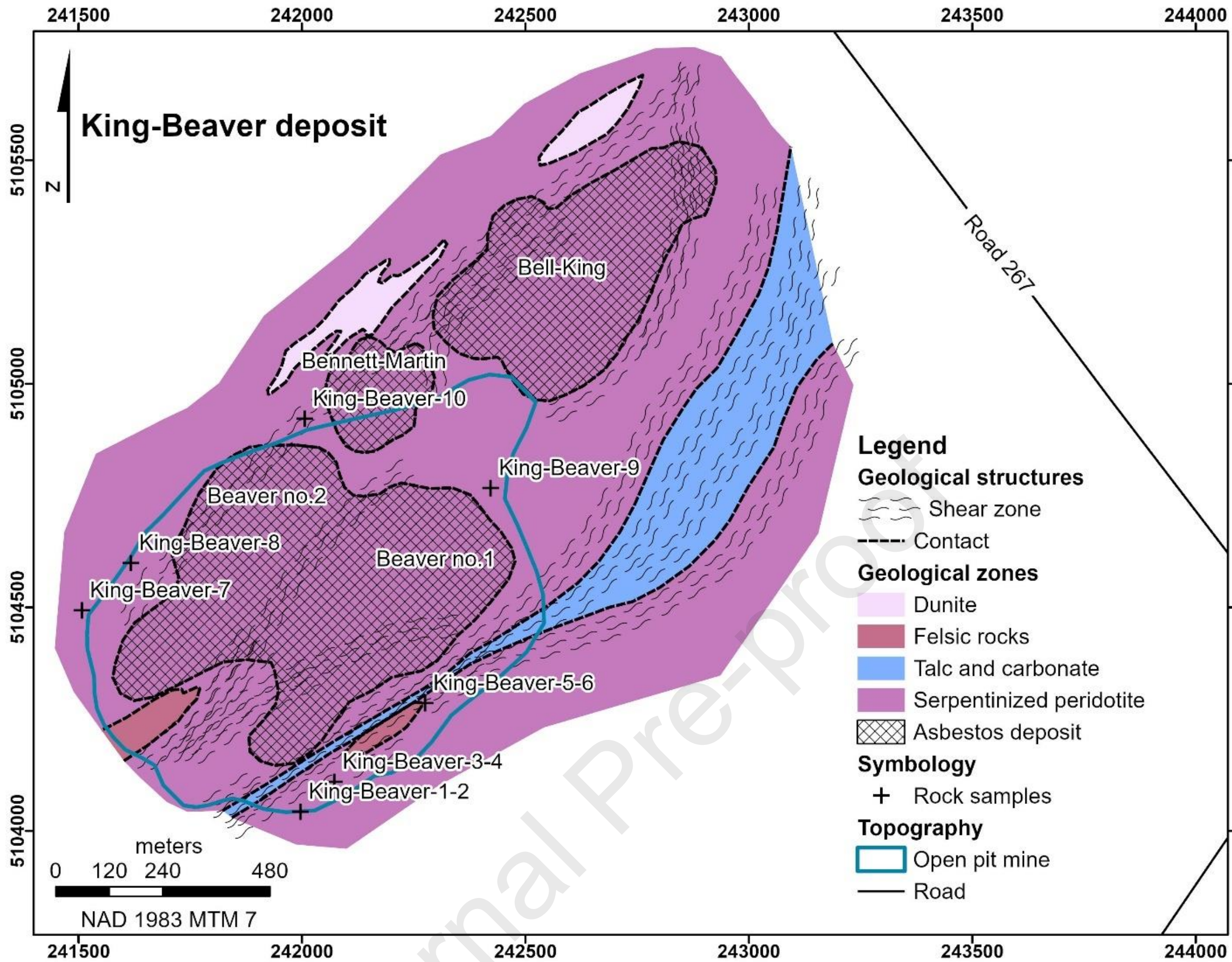

Figure 3. Bedrock geology map of the King-Beaver mine with locations of rock samples (adapted from Riordon [37]). The location of mine is shown in Figure 1.

The King-Beaver open-pit mine stands at the centre of the city of Thetford Mines (Figure 1). The Thetford Mines Ophiolite Complex sequence extends southwestward, covering approximately 55 km with a maximum width of 10 km [33]. King-Beaver mined asbestos deposits in the Thetford Mines group, representing an agglomeration of the deposits known as Bell-King, Bennett-Martin, Beaver No.1 and Beaver No.2. These deposits are separated from each other by fully serpentinized, barren peridotite that displays considerable shearing in multiple locations. Adjacent to the deposits lie various lenses of serpentinized dunite toward the northwest, with felsic rocks abundantly scattered throughout the area. Additionally, a zone featuring thrust faults is characterized by the presence of talc and carbonate, where the surrounding peridotite experienced intense crushing and shearing [37] (Figure 3).

3. SITE CHARACTERIZATION

Estimating the geothermal resources using a thermal power balance approach requires characterization of the host rock thermal properties, the groundwater and runoff temperature, the pit lake volume, and its water supplies. Below is key information obtained from site characterization, serving as input for thermal power balance calculations.

3.1 Thermal Properties of Host Rock

The sampling strategy was to collect all the geological lithologies present in order to analyze their thermal properties in the laboratory. The sampling locations (Figures 2 and 3) therefore consisted of the places where these lithologies outcrop at the surface. Thermal conductivity and diffusivity were simultaneously assessed using an infrared scanner (Thermal Conductivity Scanner; TCS), manufactured by Lippmann and Rauen. Equipped with infrared temperature sensors, this device measures thermal properties of rock samples under transient conditions. The scanner takes measurements every 2 mm along the scan line, and the sample's thermal properties are determined by the average of the measurements recorded along this trajectory [38]. Samples were prepared with flat surfaces parallel and perpendicular to the dominant foliation or schistosity, and coated with a thin layer of black paint to minimize heat diffraction effects. To validate the repeatability of the device's results, three evaluations of thermal properties were conducted on each flat surface.

At the Carey Canadian mine site, analyses involved six peridotite, eight schist and six orthoquartzite samples. Approximately 82 % of the rock surface within the mining pit comprises metasedimentary rock, while the remaining 18 % peridotite [37]. Assuming this proportion is representative over the entire pit, average thermal properties were estimated with a thermal conductivity of 3.37 $Wm^{-1}K^{-1}$, a thermal diffusivity of 1.39 mm^2s^{-1} and a volumetric heat capacity of 2.73 $MJm^{-3}K^{-1}$ (Figure 4).

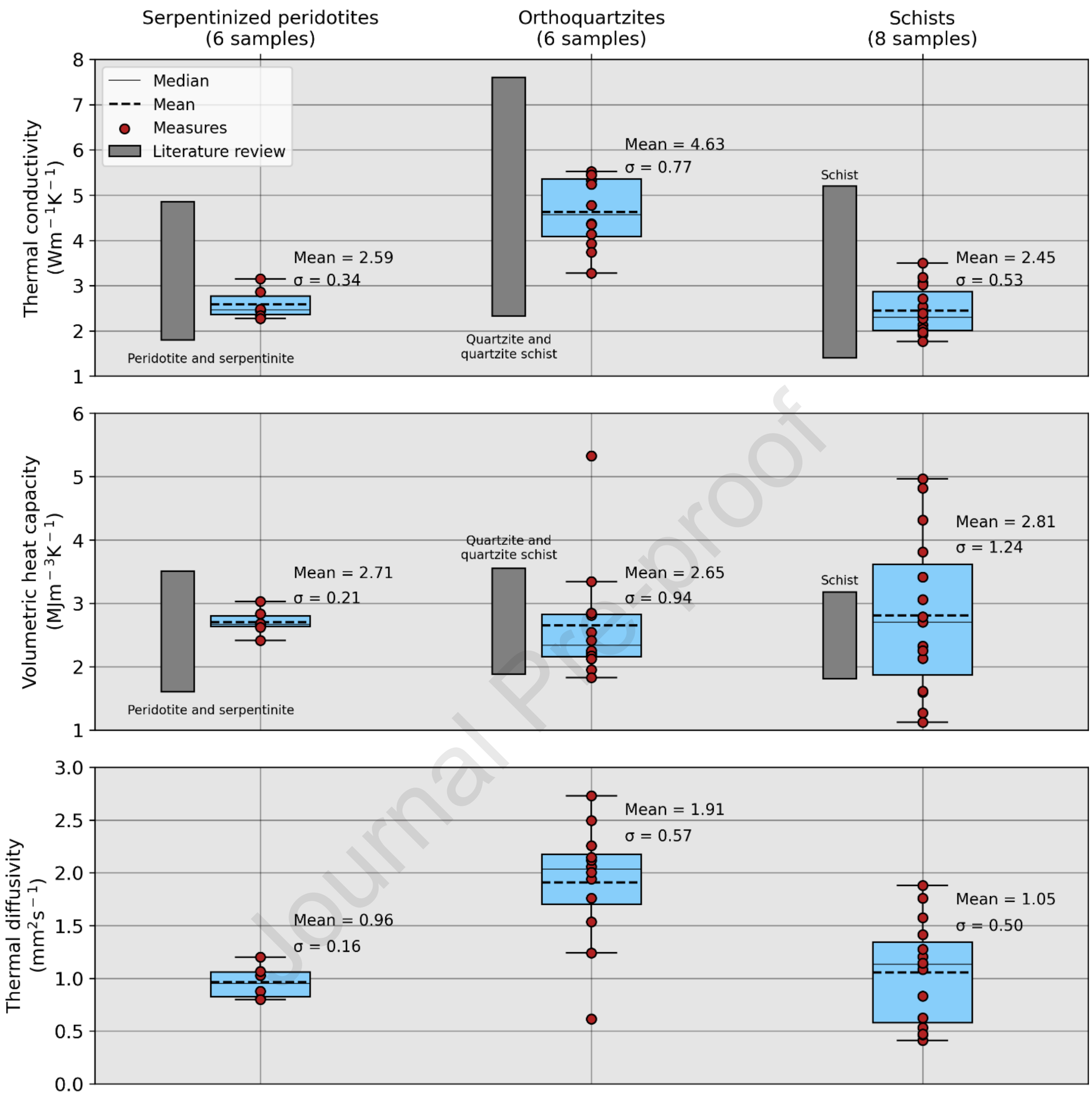

Figure 4. Thermal properties of the main lithologies sampled at the Carey Canadian mine site and analyzed in the laboratory using an infrared scanner.

Similarly, at the King-Beaver mine site, ten serpentinized peridotite samples were collected. Thermal conductivity and diffusivity were estimated at 2.74 $Wm^{-1}K^{-1}$ and 1.04 mm^2s^{-1}, respectively, with a volumetric heat capacity of 2.65 $MJm^{-3}K^{-1}$ (Figure 5).

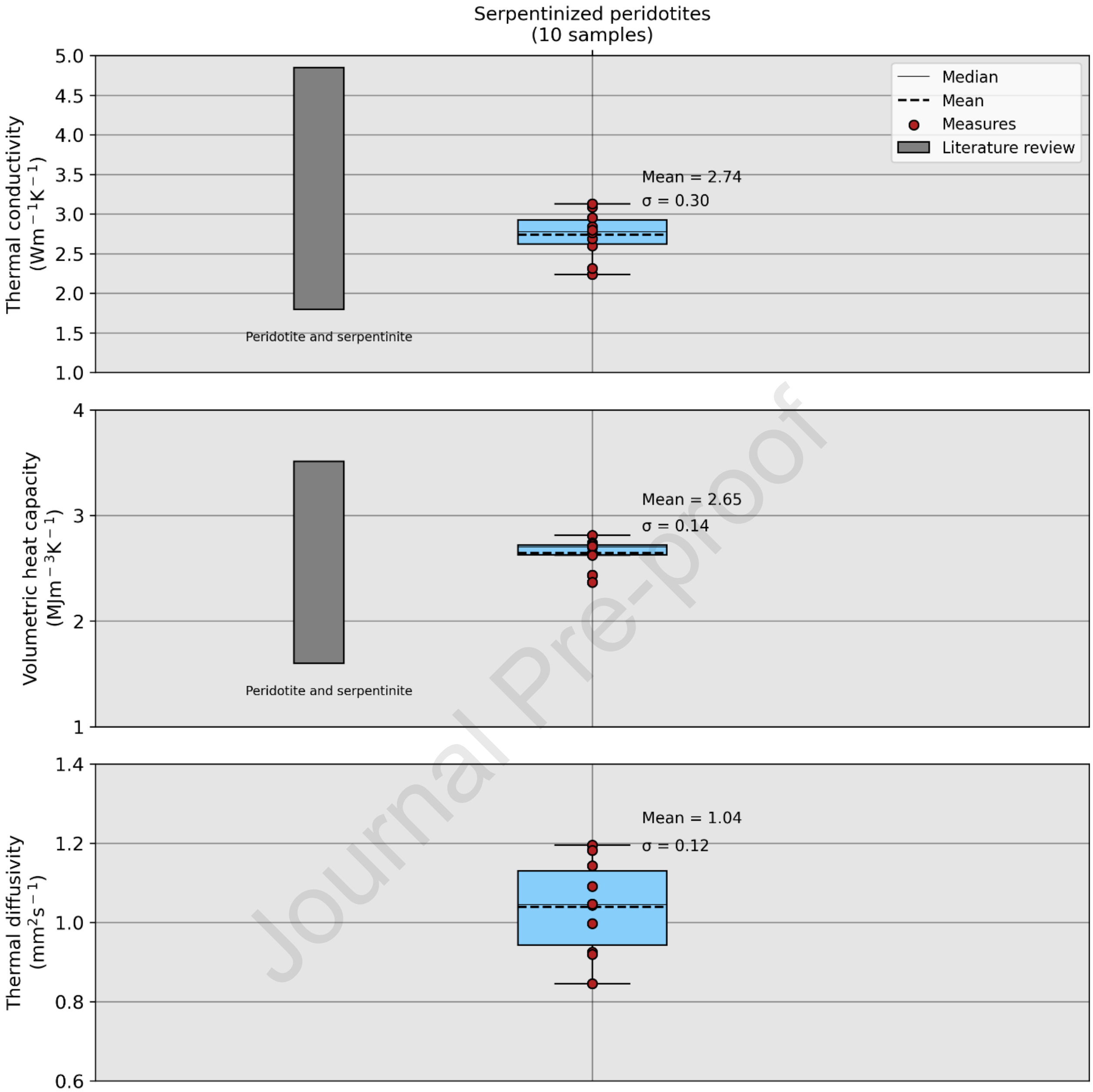

Figure 5. Thermal properties of the main lithologies sampled at the King-Beaver mine site and analyzed in the laboratory using an infrared scanner.

Laboratory values were compared with typical literature values for each lithology to ensure their consistency [39,40,41,42,43] (Figures 4 and 5).

3.2 Host Rock Temperature

To determine the host rock temperature at depth, the geothermal gradient and the surface temperature need to be known. A study conducted in Thetford Mines by Misener and Thompson [44] determined the geothermal gradient at the King-Beaver mine site to be 15.8 $°Ckm^{-1}$. This gradient was established based on eight temperature measurements taken between depths of 150 and 350 m.

We consider the undisturbed ground temperature as the surface temperature of the host rock, that remains stable throughout the year, unaffected by seasonal climate variations. Based on a study by Ouzzane et al. [45], the undisturbed ground temperature (T_{g}; K) can be estimated using a linear correlation with ambient air temperature (T_{amb}; K) :

$$T_{\mathrm{g}} = 0.9513 T_{\mathrm{amb}} + 17.898 \quad [1]$$

Considering the average annual temperature of 3.6 °C (276.15 K) for Tring-Jonction and 4.6 °C (277.15 K) for Thetford Mines, the estimated undisturbed ground temperature is approximately 7.4 °C for Carey Canadian and 8.3 °C for King-Beaver [46].

3.3 Pit Lake Volumes

In August 2022, bathymetric surveys were conducted using a sonar system mounted on a boat to systematically inspect the pit lakes. The gathered data was processed using geographic information software. The water surface area within the Carey Canadian pit spans 452,141 m^2, resulting in a water volume of 23,174,512 m^3 (Figure 6). The water surface area of the King-Beaver pit measures 476,139 m^2, with a water volume of 31,166,161 m^3 (Figure 7).

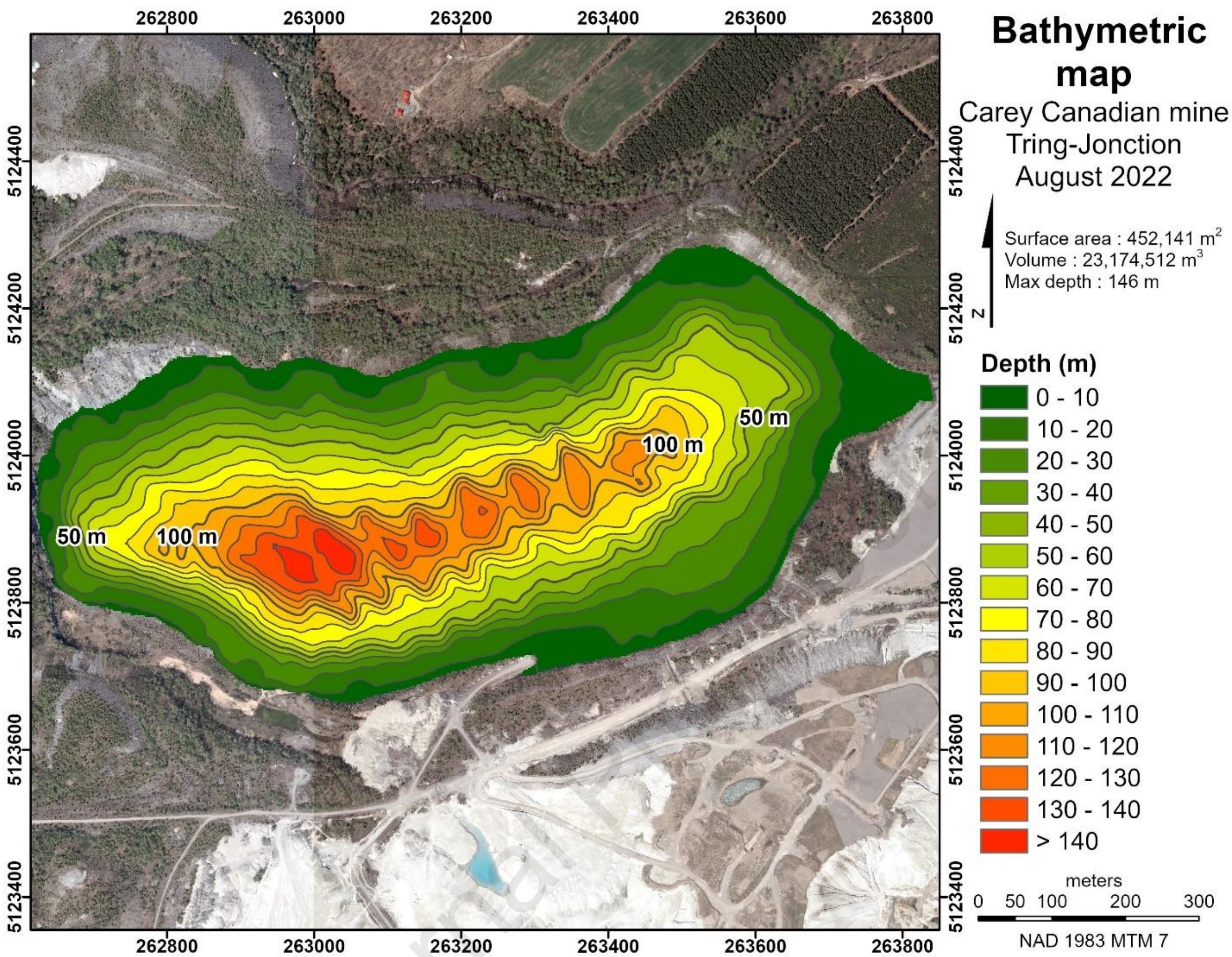

Figure 6. Bathymetric map of the Carey Canadian mine, August 2022.

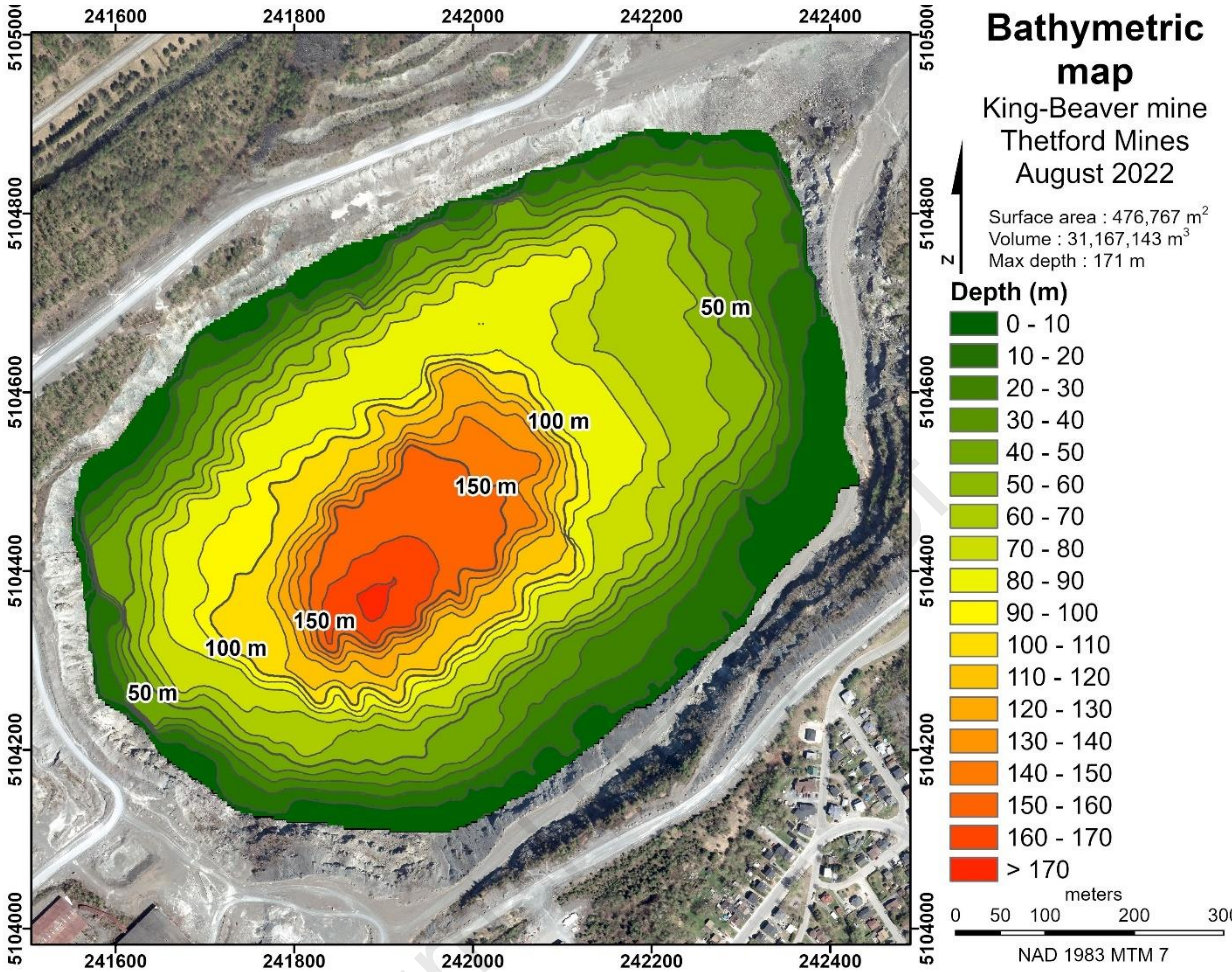

Figure 7. Bathymetric map of the King-Beaver mine, August 2022.

3.4 Pit Lake Temperature

Twelve Star-Oddi temperature sensors were vertically distributed across the 100-meter depth range in both the Carey Canadian and King-Beaver pits. These sensors recorded hourly data between November 2021 and October 2022. Each sensor generated approximately 8,760 temperature readings. Bathymetric data were used in conjunction with geographic information software to determine the volume of water between temperature sensors. The recorded temperatures were then weighted based on the respective water volume to compute the average annual temperature by depth [47].

3.5 Water Supply Volumes

The Carey Canadian and King-Beaver mine watershed were studied by estimating the annual water input derived from precipitation, runoff, and groundwater recharge. Watershed boundaries were determined with a digital terrain model (DTM) created from Lidar surveys (2018), overlaid with contour lines extracted from digital elevation models (DEM; Government of Quebec, 2014). The Thornthwaite [48] method was used to assess the hydrogeological balance. Climate data was collected from weather stations in Thetford Mines and Saint-Séverin, compiled between 1981 and

2010 [46] (Figure 8Figure 9). This methodology aligns with guidelines outlined by the Government of Quebec [49], Pédelaborde [50] and Gammons et al. [51]. Further details are provided in the appendix.

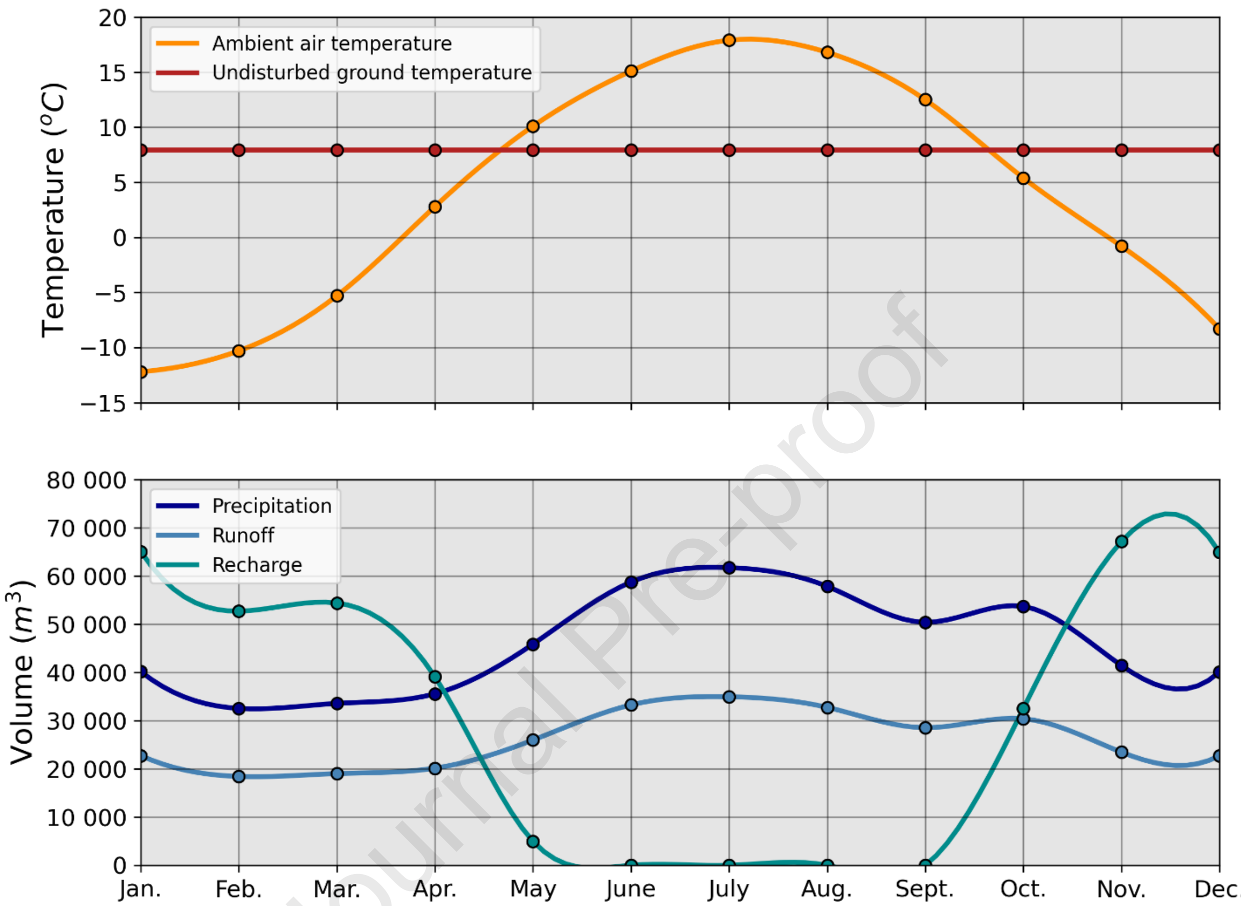

Figure 8. Water supply volumes and initial temperatures by month of the year for Carey Canadian mine watersheds [46].

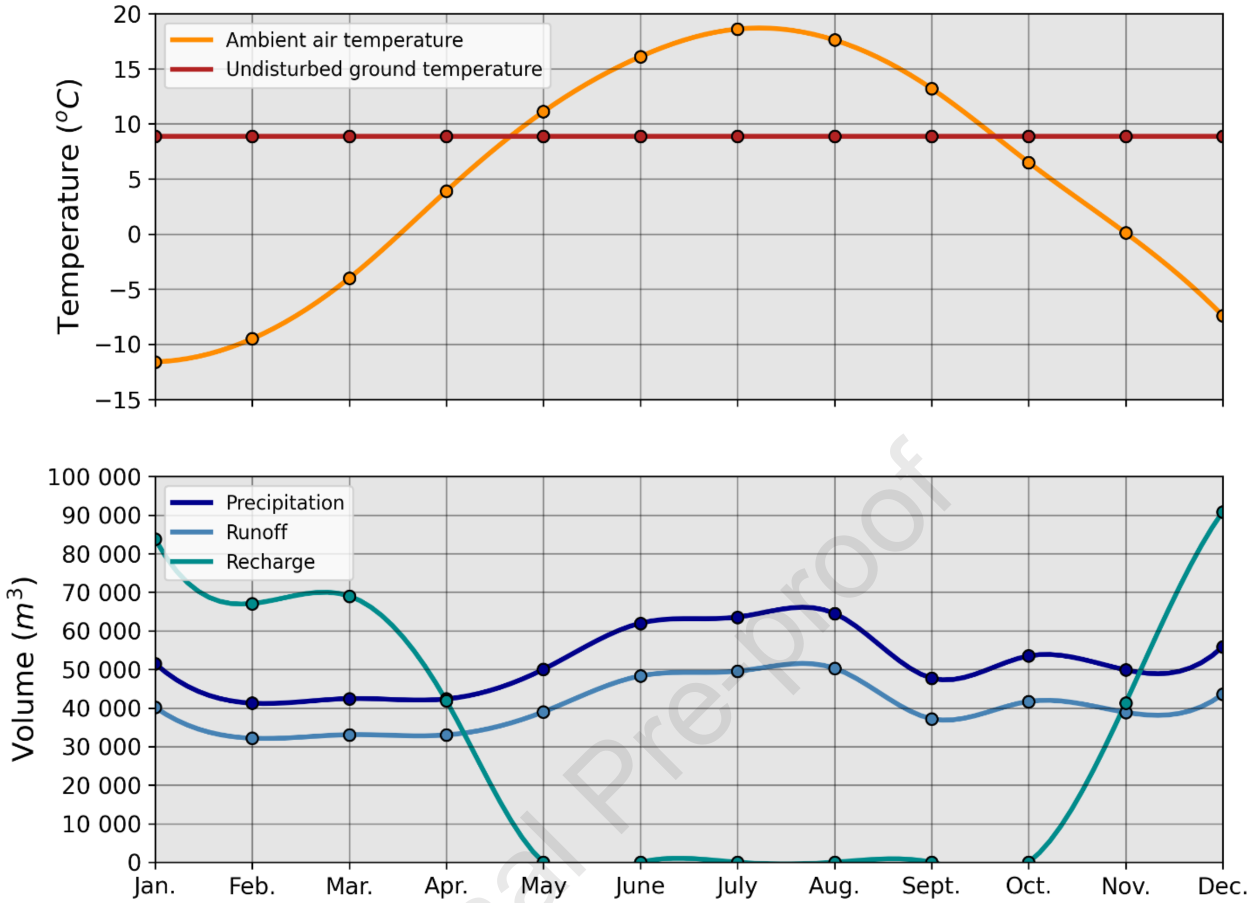

Figure 9. Water supply volumes and initial temperatures by the month of the year for King-Beaver mine watersheds [46].

4. THERMAL ENERGY AND POWER BUDGET

The results are presented in terms of thermal power (Q_{tot} : MW) and represent the ratio between available thermal energy (E : MJ) and the duration of resource exploitation (t : s).

$$Q_{\mathrm{tot}} = Q_{\mathrm{s}} + Q_{\mathrm{d}}^{\mathrm{rock}} + Q_{\mathrm{d}}^{\mathrm{supply}} = \frac{E_{\mathrm{s}} + E_{\mathrm{d}}^{\mathrm{rock}} + E_{\mathrm{d}}^{\mathrm{supply}}}{t} \qquad [2]$$

The resource estimate here is based on an assumed operational span of 25 years, which aligns with the minimum anticipated lifespan of a GHP system.

The proposed thermal power balance to assess the geothermal resource of a flooded open-pit mine considers the static energy within the water volume of the pit lake (Q_{s} : MW), as well as the dynamic energy recharge by heat conduction from the host rock ($Q_{\mathrm{d}}^{\mathrm{rock}}$: MW) and energy contributions from water supplies (precipitation, runoff and groundwater recharge; $Q_{\mathrm{d}}^{\mathrm{supply}}$: MW). Evaporation, solar radiation, wind, terrestrial heat flux, and natural or forced convection resulting from water movements have been neglected for simplifications (Figure 10).

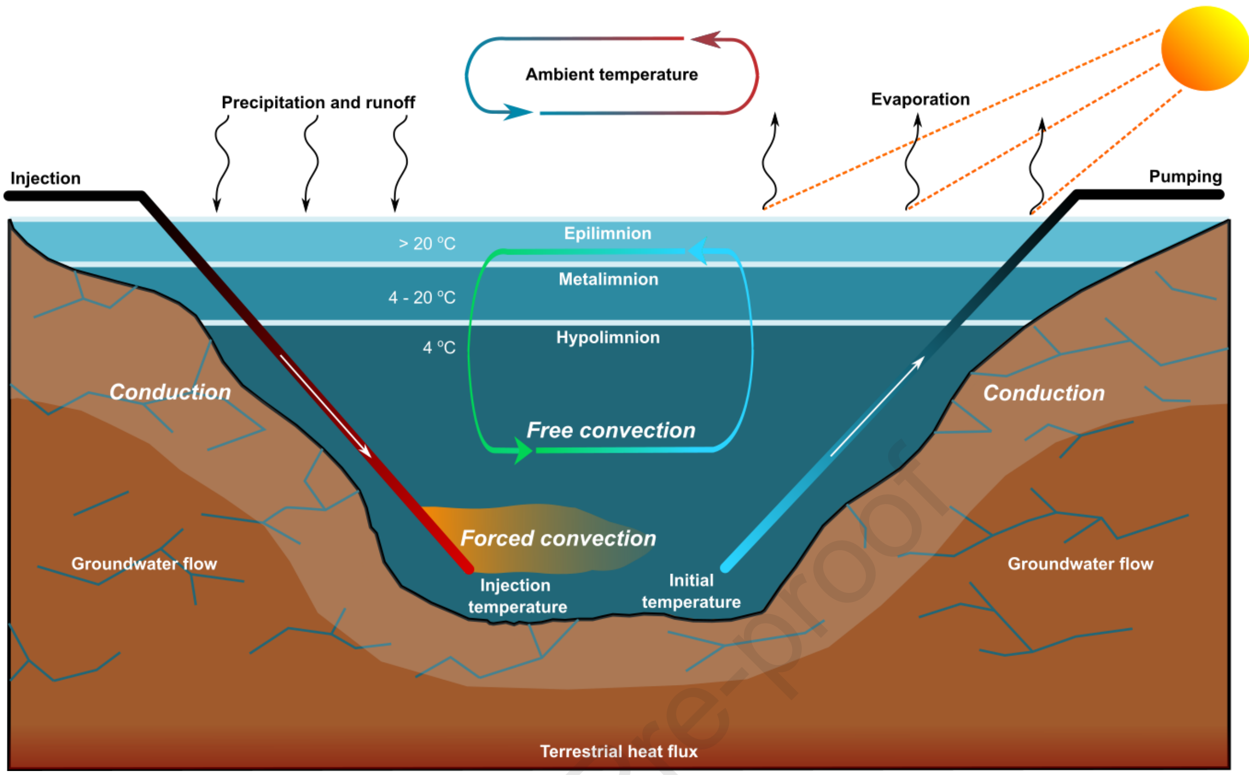

Figure 10. Conceptual model of the main heat transfer mechanisms between the environment of a pit lake with the operation of a geothermal system (adapted from Chiasson [52] and RAPPEL [53]).

4.1 Static Energy Contained in the Pit Lake

The estimate of static energy (E_s ; MJ) is made with the volume method of assessing the thermal energy provided by a stationary water volume [14,17,54]. This approach relies on the volume of water within a basin (V_w ; m^3), the volumetric heat capacity of water (c_w = 4.184 MJm^{-3}K^{-1}), and the difference between its mean annual temperature (T_w ; °C or K) and its final temperature (T_f ; °C or K) post thermal energy extraction or injection:

$$E_s = V_w c_w (T_w - T_f) \qquad [3]$$

4.2 Dynamic Energy Contribution of the Host Rock

Upon cooling or heating, the host rock, and the pit lake will exchange heat by conduction. The energy contribution from the host rock can also be assessed using the volume method. This estimation evaluates the volume of rock affected by temperature fluctuations induced by direct contact with water. The process of heat transfer from water to host rock is assumed representative of heat conduction in a semi-infinite solid medium. This simplification implies the rock is represented by a solid with a distinct surface that extends to infinity in outward pit directions. When subjected to abrupt changes in surface temperature conditions, the solid undergoes nearly one-dimensional transient conduction [55]. The fundamental transient conductive heat transfer equation for a semi-infinite solid is described by:

$$\frac{\partial^2 T}{\partial^2 x} = \frac{1}{a}\frac{\partial T}{\partial t} \quad [4]$$

In scenarios where the surface conditions are defined by a constant temperature, the initial conditions are expressed as:

$$T(x,0) = T_{\text{init}} \quad [5]$$

$$T(0,t) = T_{\text{f}} \quad [6]$$

and the boundary condition within the solid is specified as:

$$T(x \to \infty, t) = T_{\text{init}} \quad [7]$$

The spatiotemporal evolution of the solid medium temperature ($T_{(x,t)}$; °C or K) is estimated using this analytical solution [55] (Figure 11):

$$T_{(x,t)} = (T_{\text{init}} - T_{\text{f}})erf\left(\frac{x}{2\sqrt{\alpha t}}\right) + T_{\text{f}} \quad [8]$$

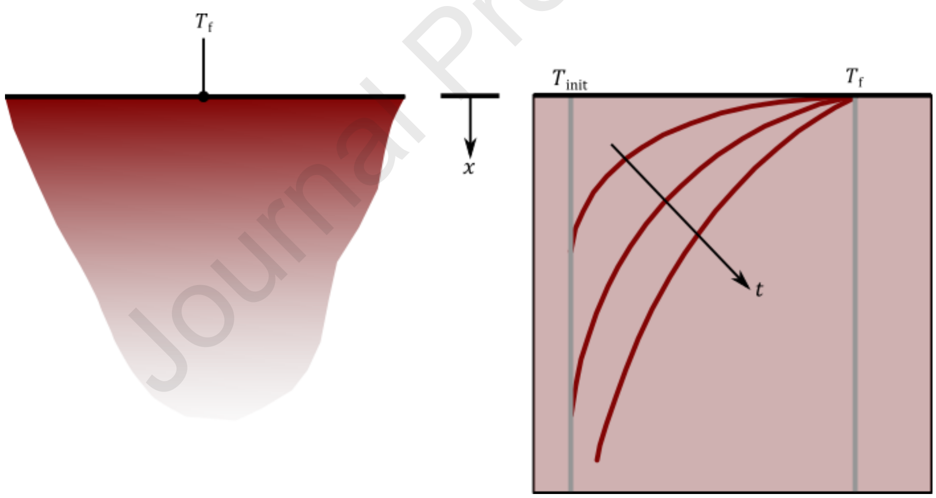

Figure 11. Transient temperature distribution in a semi-infinite solid when surface conditions correspond to a constant temperature.

This equation depends on time (t ; s), thermal diffusivity of the solid (α ; m^2s^{-1}), distance within the solid medium from its surface (x ; m), the temperature difference between the initial temperature of the solid medium (T_{init} ; °C or K) and temperature change applied to its surface (T_{f} ; °C or K).

The geometry of an open-pit mine can be represented by a half-ellipsoid shape whose volume is equivalent to the volume of water contained within the pit. This geometry has three axes: x and y represent the pit's horizontal components, and z the vertical component, respectively. Heat transfer analysis needs to be conducted for each of these axes since the initial rock temperature acts as a boundary condition and varies according to the spatial component of the half-ellipsoid. The boundary condition applied to calculate conductive heat transfer for the horizontal components (x and y) assumes a fixed temperature. This temperature is considered equivalent to the mean annual water temperature (T_w), since it is assumed that in the initial state, the host rock is in thermal equilibrium with the water temperature.

$$T_{init} = T_w \quad [9]$$

However, rock temperature (T_r) varies with depth according to a geothermal gradient (dT/dz). Consequently, the initial temperature of the rock increases in relation to depth, defined by this equation:

$$T_r = T_w + \left(\frac{dT}{dz}\right) z \quad [10]$$

As a result, the boundary condition for computing heat transfer between water and rock at the horizontal components (x and y) is:

$$T(xy \to \infty, t) = T_w \quad [11]$$

The boundary condition for computation at the vertical component (z) is represented by this assumption:

$$\text{if } \left(T_r - T_{(z,t)}\right) \leq 0.05 \text{ then } T_{(z,t)} = T_r \quad [12]$$

If the rock surface temperature increases, the distance of temperature propagation along the horizontal axes of the pit is expected to be greater than the propagation distance along the vertical axis (Figure 12).

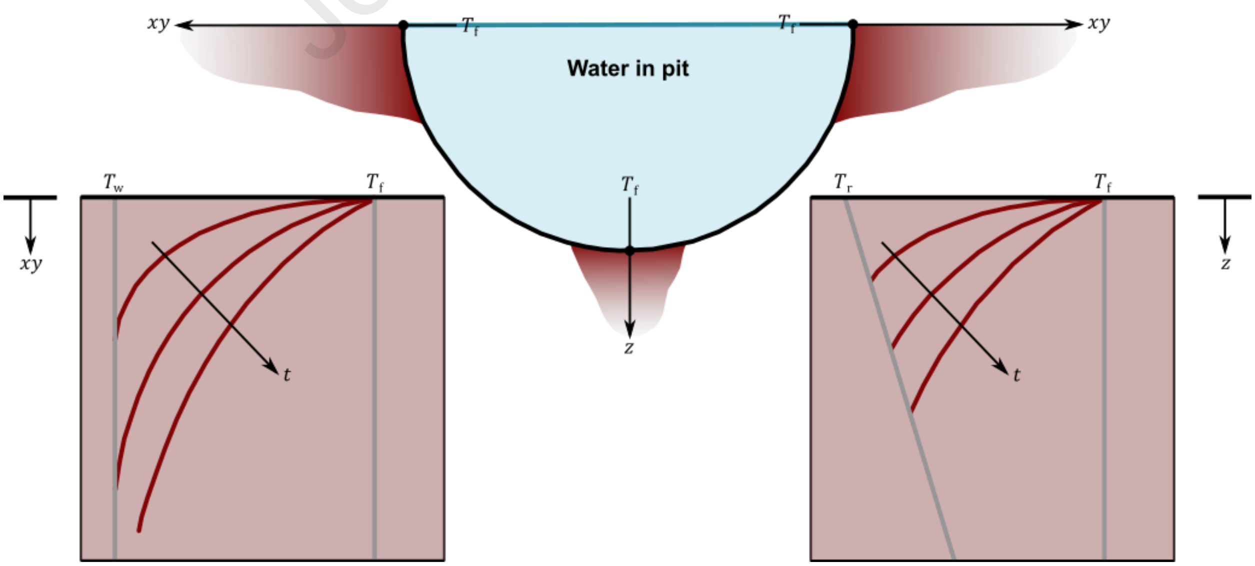

Figure 12. Transient temperature distribution in a semi-infinite solid when boundary conditions vary spatially considering a sudden increase in surface temperature (inspired by Incropera et al. [55]). The bottom left box shows

lateral temperature changes (XY) within the host rock, which tend to reach equilibrium with the initial water temperature. On the right, the temperature changes in depth (Z) tend to reach equilibrium based on the geothermal gradient, hence the inclined line.

The opposite effect is anticipated when the surface temperature is suddenly lowered. In this scenario, a decrease in the rock surface temperature results in a shorter propagation distance along the pit's horizontal axis compared to the vertical axis. However, heat recovery in abandoned and flooded open-pit mines is subject to lower temperature differences compared to instances of free cooling or cooling applications because temperatures below the thermocline are relatively cold [51]. Consequently, the impact of the geothermal gradient on temperature propagation distance is significantly diminished during warming as compared to its effect during cooling applications. Due to this, it becomes feasible to impose a fixed temperature, equivalent to the mean annual water temperature, as a boundary condition on the vertical component to represent heat extraction (Figure 13).

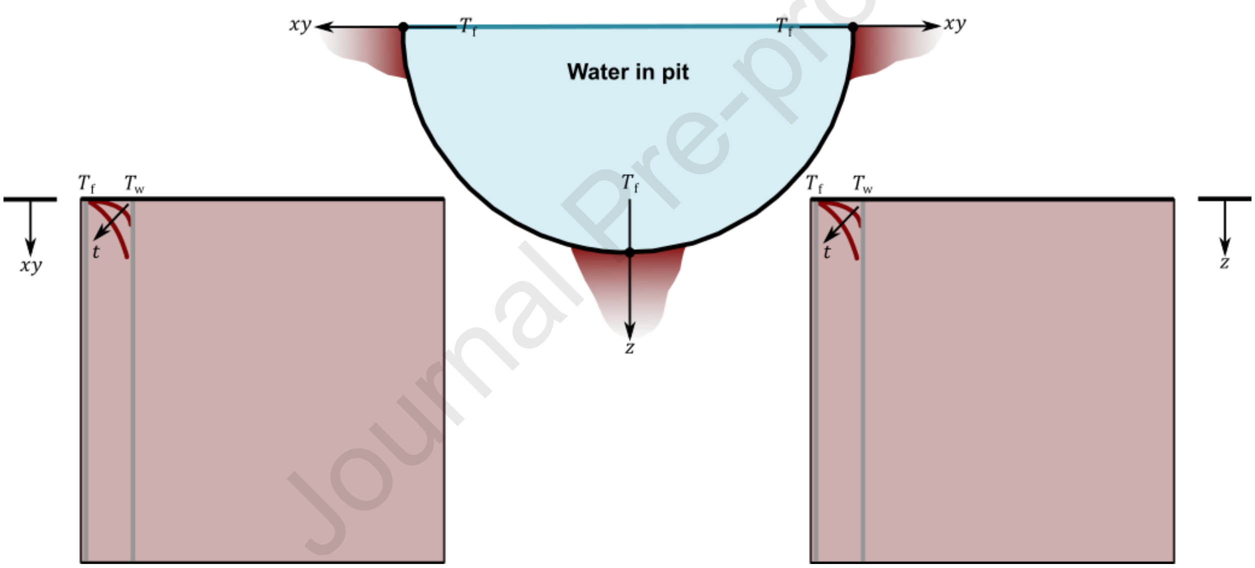

Figure 13. Transient temperature distribution in a semi-infinite solid when boundary conditions vary spatially considering a sudden decrease in surface temperature (inspired by Incropera et al. [55]).

The maximum distance of temperature propagation across the three axes of the initial half-ellipsoid is summed to estimate the rock volume considered in the thermal balance calculation. The maximum distance of temperature propagation is reached when the difference between the calculated temperature as a function of the distance and the initial temperature of the rock is nearly zero:

$$xy_{\max} : T_{(xy,t)} \simeq T_{\mathrm{w}} \qquad [13]$$

$$z_{\max} : T_{(z,t)} \simeq T_{\mathrm{r}} \qquad [14]$$

This method allows determining the volume of rock affected by temperature variations by subtracting the volume of water from the total volume (volume of water and rock; Figure 14).

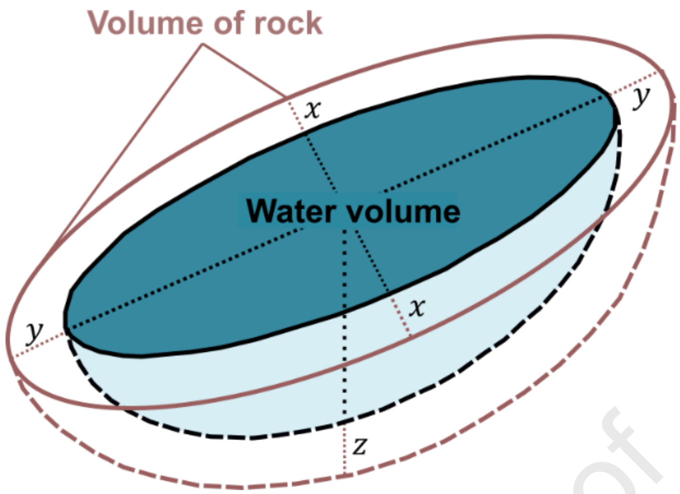

Figure 14. Open-pit geometry simplified by a half-ellipsoid form for estimating the volume of rock impacted by water temperature variations.

The amount of energy extracted from the host rock diminishes with distance, as beyond the affected rock thickness, the rock temperature gradually approaches its initial temperature. The temperature can be determined at multiple points to evaluate the variation in energy contribution provided by the host rock as a function of distance. For this purpose, the volume of rock affected by temperature variations (V_r^i ; m^3) is segmented into n bands, each assuming a constant temperature ($T_{(x,t)}^i$; °C or K). The total estimated energy contribution supplied by the rock ($E_\mathrm{d}^\mathrm{rock}$; MJ) is the sum of available energy within these bands:

$$E_\mathrm{d}^\mathrm{rock} = \sum_{i=1}^{n} V_\mathrm{r}^i c_\mathrm{r} \left(\frac{T_\mathrm{r} - T_{(x,t)}^i}{2} \right) \qquad [15]$$

In this equation, c_r (MJm^{-3}K^{-1}) represents the volumetric heat capacity of the solid medium. In this approach, it is assumed that water temperature changes suddenly. However, when considering a constant heat or cold injection, the pit water temperature will gradually increase or decrease over the operating period to ultimately reach the final temperature. Thus, a more representative calculation should determine the average energy contribution. Given that V_r^i and c_r represents constant variables for each of the n bands, the energy becomes a linear function of ΔT. Consequently, the average energy contribution is determined by $\Delta T/2$, which represents the average temperature over the course of 25 years.

4.3 Dynamic Energy Contribution of the Water Supply

The assessment of the energy contribution from water supply ($E_\mathrm{d}^\mathrm{supply}$; MJ) in the mining pits can also be computed using the volume method. This corresponds to the sum of the energy provided by precipitation on the pit lake's surface (E_P ; MJ), runoff water (E_R ; MJ) and groundwater recharge (E_G ; MJ):

$$E_{\mathrm{d}}^{\mathrm{supply}} = E_{\mathrm{P}} + E_{\mathrm{R}} + E_{\mathrm{G}} \qquad [16]$$

The energy provided by precipitation can be evaluated using this equation:

$$E_{\mathrm{P}} = \sum_{i=1}^{12} V_{\mathrm{P}}^{i} c_{\mathrm{w}} \left(T_{\mathrm{amb}}^{i} - T_{\mathrm{f}}\right) \qquad [17]$$

Here, V_{P}^{i} (m^3) represents the monthly height of the water column precipitated, multiplied by the surface area of the water within the pit lake. The initial temperature of the precipitated water is considered equivalent to the monthly ambient air temperature (T_{amb}^{i}; °C). Note that these calculations are made for each month, denoted by the exponent i (Figure 8Figure 9). It is also important to note that negative temperatures are capped at 0 °C.

The assessment of the energy provided by runoff is calculated similarly:

$$E_{\mathrm{R}} = \sum_{i=1}^{12} V_{\mathrm{R}}^{i} c_{\mathrm{w}} \left(T_{\mathrm{amb}}^{i} - T_{\mathrm{f}}\right) \qquad [18]$$

Here, V_{R}^{i} (m^3) represents the monthly height of the runoff water column, multiplied by the total surface area of the watershed. Similarly, the initial temperature of the runoff water is considered equivalent to the monthly ambient air temperature (T_{amb}^{i}; °C) of the area (Figure 8Figure 9). Again, negative temperatures are capped at 0 °C.

Finally, the energy provided by the quantity of infiltrated water can be determined using the following equation:

$$E_{\mathrm{G}} = \sum_{i=1}^{12} V_{\mathrm{G}}^{i} c_{\mathrm{w}} \left(T_{\mathrm{g}} - T_{\mathrm{f}}\right) \qquad [19]$$

Here, V_{G}^{i} (m^3) represents the monthly height infiltrated water column, multiplied by the total surface area of the watershed. The initial groundwater temperature is associated with the undisturbed ground temperature (T_{g} ; °C; Figure 8 Figure 9), typically found at depths of 10 meters or more, remaining stable year-round.

4.4 Available Thermal Power for Buildings

The thermal power supplied to buildings (Q_{b} ; MW) by a GHP depends on the end-use (heating or cooling) and can be estimated considering the heat pump coefficient of performance (COP) using the following equations [56]:

$$Q_{\mathrm{b}} = \frac{Q_{\mathrm{tot}}\left(COP_{\mathrm{heating}}\right)}{COP_{\mathrm{heating}} - 1} \qquad [20]$$

$$Q_{\mathrm{b}} = \frac{Q_{\mathrm{tot}}\left(COP_{\mathrm{cooling}}\right)}{COP_{\mathrm{cooling}} + 1} \qquad [21]$$

A reduction in the average annual water temperature down to 2 °C is considered in the evaluation of the geothermal potential of pit lakes for heating buildings. In contrast, an increase in average annual water temperature from 15 up to 40 °C is considered in the cooling potential assessment. A COP for these temperature ranges is 3.30 for heating buildings and 4.30 for cooling purposes [7], which is typical of heat pump system efficiency. Direct cooling without the use of a heat pump can also be achieved but with a lower maximum temperature considered to be 15 °C and is referred here as free cooling. In this case, the thermal power supplied to buildings is equal to the total thermal power injected in the mine site.

5. RESULTS

Aside from the monthly variations of water supplies and ambient temperature presented in the site characterization section (Figure 8 Figure 9), all the inputs required to calculate the thermal power balance for the Carey Canadian and King-Beaver mines can be represented with eight simple parameters (Table 1).

Table 1. Parameters used to calculate the thermal power balance for the Carey Canadian and King-Beaver mines.

Parameters	Symbols	Carey Canadian	King-Beaver	Units
Available water volume	V_{w}	23,174,512	31,167,143	m^3
Initial water temperature	T_{w}	5.23	5.35	°C
Undisturbed ground temperature	T_{g}	7.94	8.89	°C
Geothermal gradient	dT/dz	0.0158		$°Cm^{-1}$
Volumetric heat capacity of water	c_{w}	4.184		$MJm^{-}3K^{-1}$
Volumetric heat capacity of host rock	c_{r}	2.73	2.65	$MJm^{-3}K^{-1}$
Thermal diffusivity of host rock	α	1.39	1.04	mm^2s^{-1}
Operating time	t	25	25	yr

The estimate of the total thermal power for buildings supplied by open-pit mines considers both static and dynamic energies, over a final water temperature range from 2 °C to 40 °C (Figure 15).

Assessment of the rock energy contribution is closely linked to the thermal energy supplied by the water volume, as the initial temperature of the rock in contact with the water is assumed to be in equilibrium with the mean annual water temperature. Based on this assumption, the energy contribution of the rock is considered to be zero when the final water temperature remains unchanged. However, the computation of the water supply energy contribution is independent of the average annual temperature of the water contained in the mining pit. As described, the initial temperature of water from precipitation and runoff is assumed to be equivalent to the ambient air temperature. Energy potential therefore varies according to the time of year. However, the energy potential of groundwater recharge is zero when the final temperature is equivalent to the undisturbed ground temperature, which remains unaffected by seasonal changes (Figure 16).

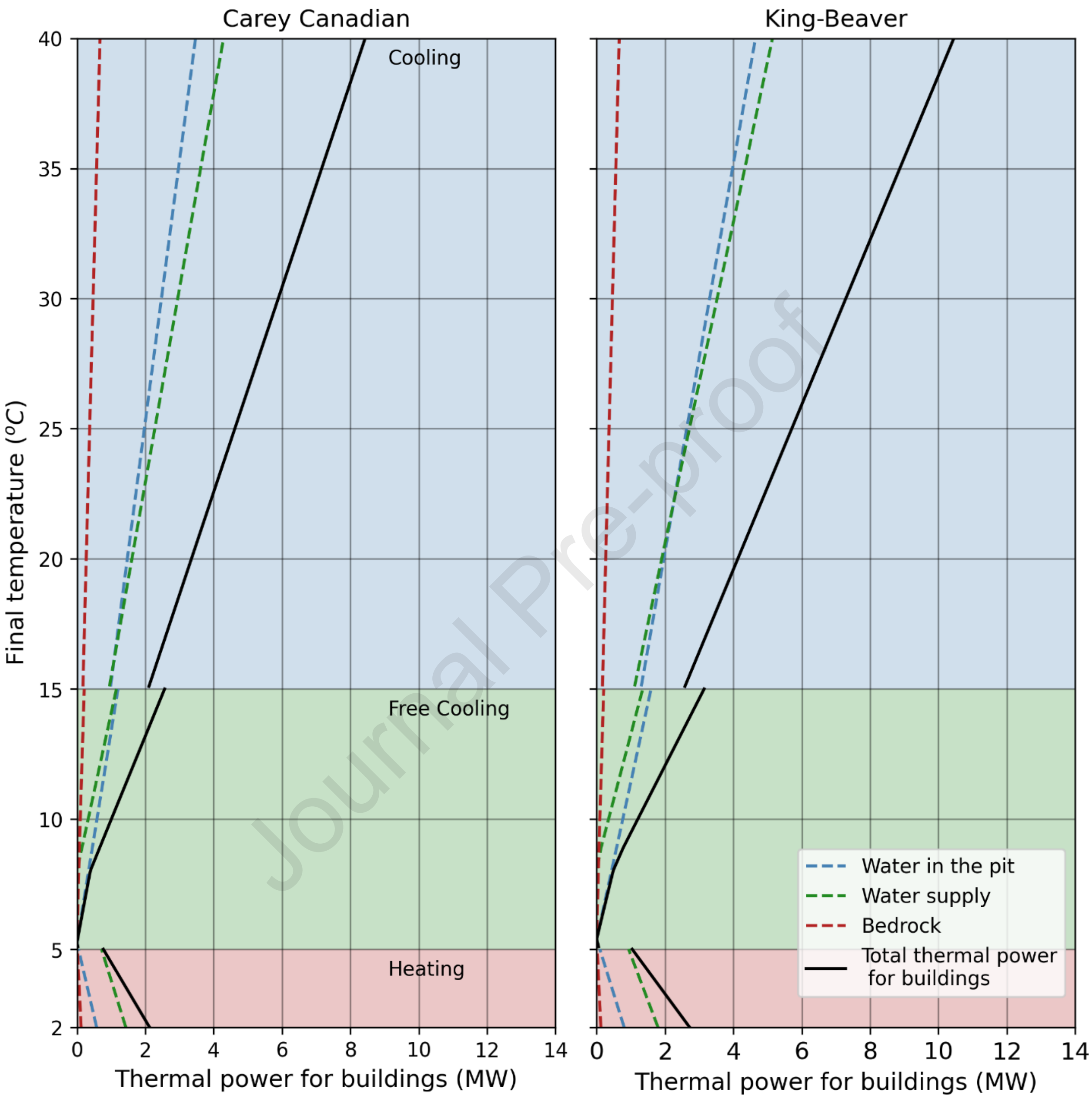

Figure 15. Total thermal power for buildings available for the abandoned and flooded Carey Canadian and King-Beaver mines as a function of final temperature.

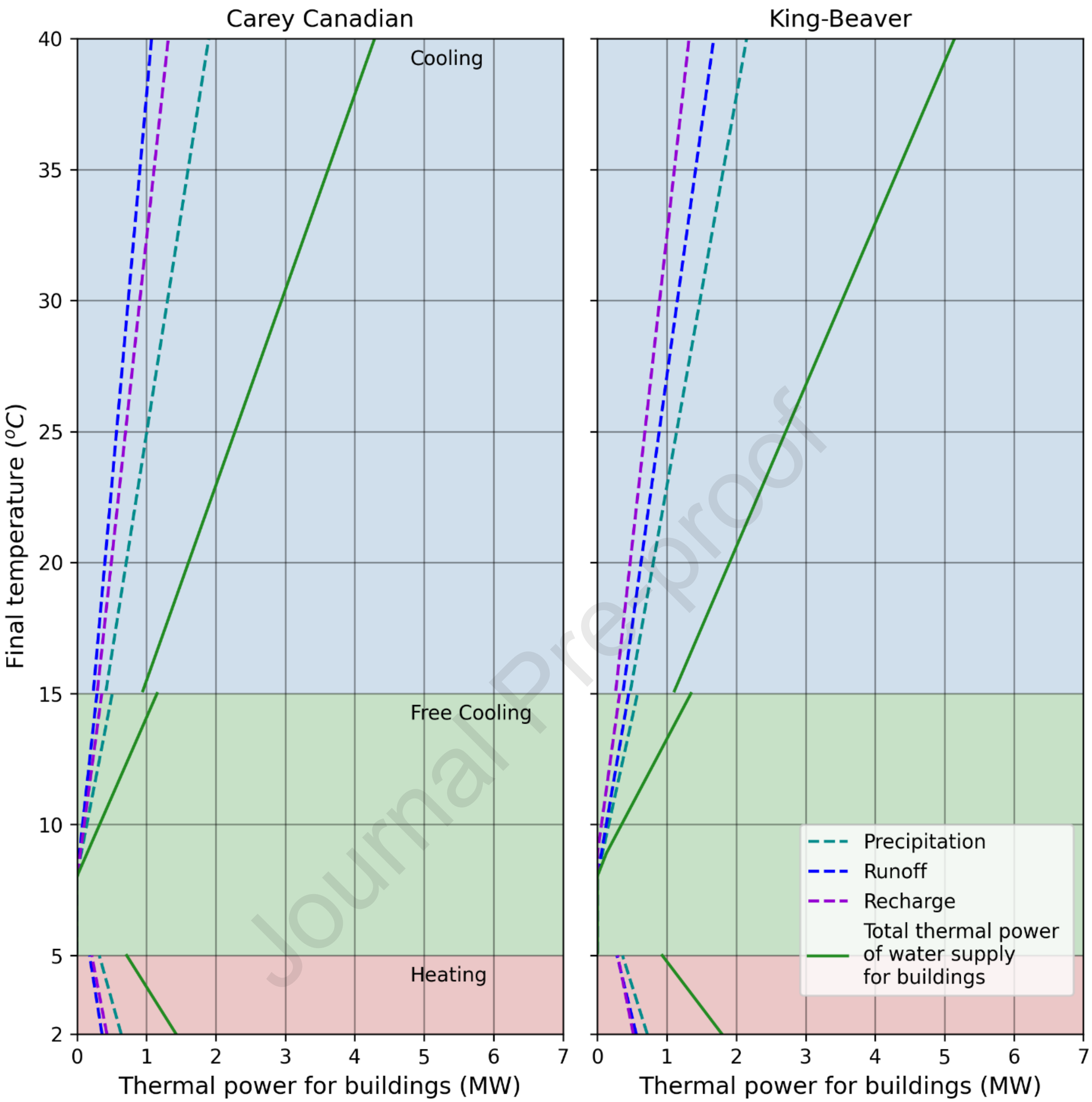

Figure 16. Thermal power contribution of water supply for buildings assessed for Carey Canadian and King-Beaver mines watershed as a function final temperature.

Each graph in figures 15 and 16 shows a curve break at 5 °C and 15 °C. These thresholds mark the transition between heating, free cooling and cooling modes. This discontinuity is due to the specific integration of COP in the calculations of the thermal power available for buildings. In heating mode, this integration enhances energy efficiency, whereas in the cooling mode, it leads to a reduction.

6. DISCUSSION

Comeau et al. [57] was the first to include a contribution from the host rock to the heat balance calculation of an open-pit mine. Using Ngoyo Mandemvo's [58] numerical simulations of the King-Beaver mine, the radius of influence for each degree of temperature change in the country rock was used to calculate the volume of rock involved per 5-meter-thick layer analytically. Ngoyo Mandemvo [58] assessed the maximum 25-year extraction of thermal energy for heating, free-cooling and cooling modes by simulating heat transfer by thermal conduction and natural convection in the surrounding rock and pit water. A heat flux of 0.044 W/m^2 is used as the basis for the 3D model, and implies heat exchange by natural convection between the water and ambient air according to local meteorological data. The present study has a slightly more accurate calculation of the surrounding rock compared to Comeau et al. [57], as it takes into account the geothermal gradient, thus slightly changing the temperature at depth. More importantly, a computer code was created to accurately calculate the volume of rock involved and the associated changes in temperature as a function of the volume and shape of a half-ellipsoid representing the volume of water in the open pit. Conversely, the temperature influence radii in the host rock used by Comeau et al. [57] apply only to the dimensions of the King-Beaver mine. Nevertheless, previous studies did not propose a method to incorporate dynamic thermal energy contributions into pit lake heat balance. Results of previous assessments of the thermal power available for buildings provided by the geothermal potential of the King-Beaver open-pit mine for heating, free cooling and cooling purposes are detailed in the Table 2. The disparity between the previous and current results can be explained, among other things, by the inclusion of water supply in the thermal power balance calculation and the lake is still filling up without having reached its maximum level yet. Indeed, the recent bathymetric surveys made in 2022 determined the available water volume to be 31,167,143 m^3, revealing an estimate almost 40 % higher than the 2019 estimate of approximately 22,635,803 m^3 used in previous studies. For a more accurate comparison with Comeau et al. [57] and Ngoyo Mandemvo [58] results, disregarding the water supply's contribution, considering an identical volume of available water and consistent initial water temperature is preferable (Table 2).

Table 2. Comparison of the geothermal potential of the King-Beaver mine between [57], [58] and the present study.

<table>
<tr><th rowspan="2">Reference</th><th rowspan="2">Approach</th><th colspan="3">Modes of use</th><th rowspan="2">Parameters considered</th></tr>
<tr><th>Heating (= 2 °C) (MW)</th><th>Free cooling (= 11 °C) (MW)</th><th>Cooling (= 20 °C) (MW)</th></tr>
<tr><td>Comeau et al., (2019)</td><td>Analytical 5-m layers</td><td>0.58</td><td>0.78</td><td>1.55</td><td rowspan="3">• Pit water volume: 22,635,803 m^3
• Host rock</td></tr>
<tr><td>Ngoyo Mandemvo, (2019)</td><td>Numerical 3D</td><td>1.97</td><td>2.00</td><td>4.43</td></tr>
<tr><td rowspan="2">Present study</td><td rowspan="2">Analytical Fine layers</td><td>0.57</td><td>0.85</td><td>1.71</td></tr>
<tr><td>2.53</td><td>2.28</td><td>4.43</td><td>• Pit water volume: 31,167,143 m^3
• Host rock
• Water supplies</td></tr>
</table>

This comparison highlights the complexity of the proposed analytical approach for evaluating the host rock's contribution. Unlike calculations of static thermal energy and the water supply contribution, estimating the energetic contribution of the host rock can require considerable computation time. Given its close correlation with the thermal energy supplied by the available water volume in the pit lake, the rock's energy contribution can be approximated as a fraction of the static energy (Figure 17).

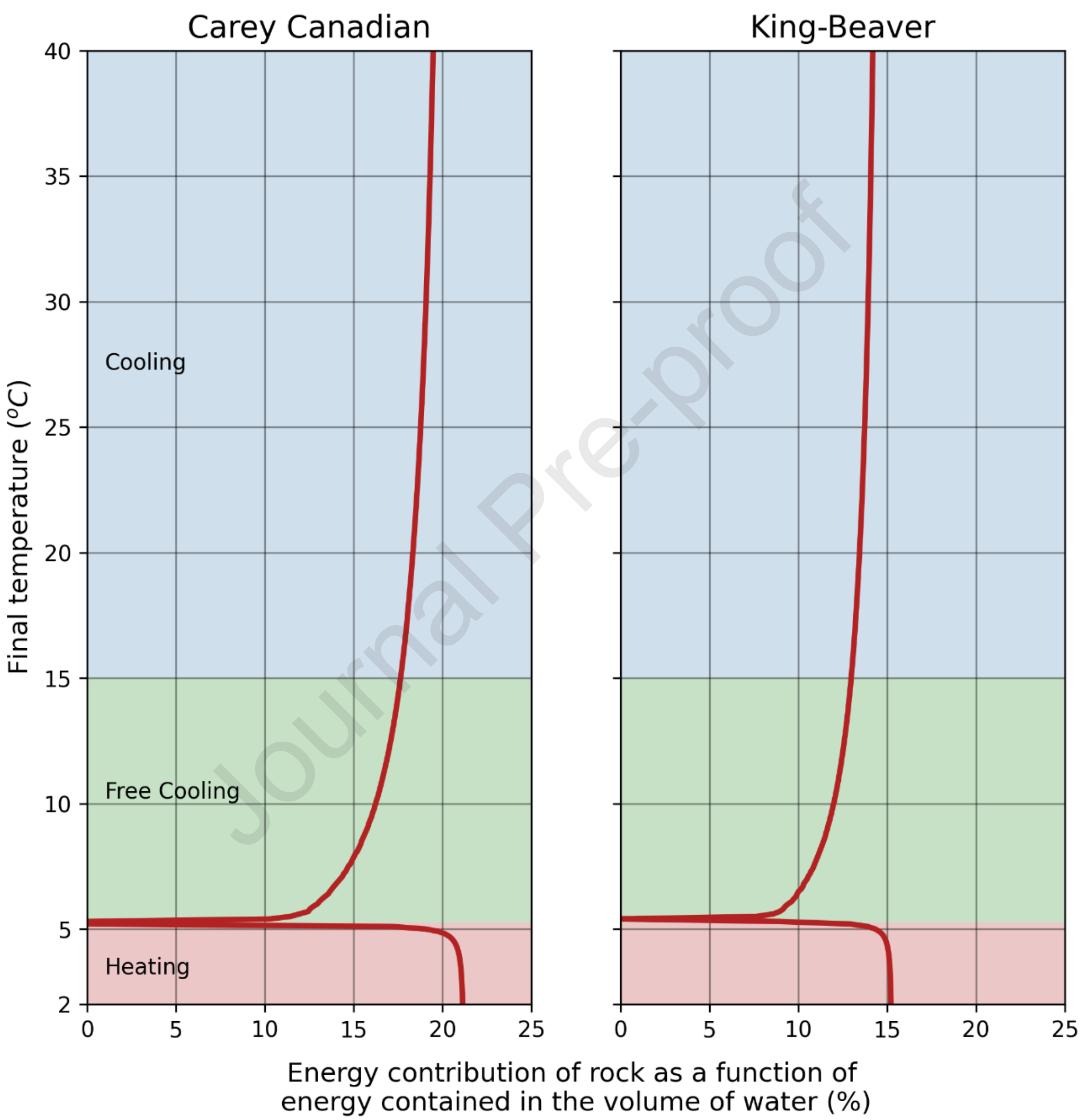

Figure 17. Estimation of the energy contribution of the host rock based on the thermal energy contained in the water volume of the Carey Canadian and King-Beaver pits.

The calculation of rock energy contribution depends on five main variables: 1) available water volume (or more precisely, the contact surface between water and rock), 2) the rock volumetric heat capacity, 3) rock thermal diffusivity, 4) geothermal gradient, and 5) temperature difference between water body and host rock. Disregarding temperature, a sensitivity analysis of parameters was conducted to better understand the influence of these variables on the amount of potential thermal energy that can be supplied by the surrounding rock. Then, values for available water volume, thermal properties, and geothermal gradient were adjusted within ± 25 % of their initial values. This arbitrary value serves as a good benchmark for sensitivity analysis, helping assess the impact of variables on the potential thermal energy from surrounding rock. While another value could have been chosen, it wouldn't alter the ranking of the most influential input parameters. Thereby, the percentage deviation is calculated by comparing the initial thermal energy estimated at a final temperature of 25 °C for the Carey Canadian and King-Beaver mines with the thermal energy obtained following parameter variation. Results are comparable for both mines and are illustrated with the average percentage deviation (Figure 18).

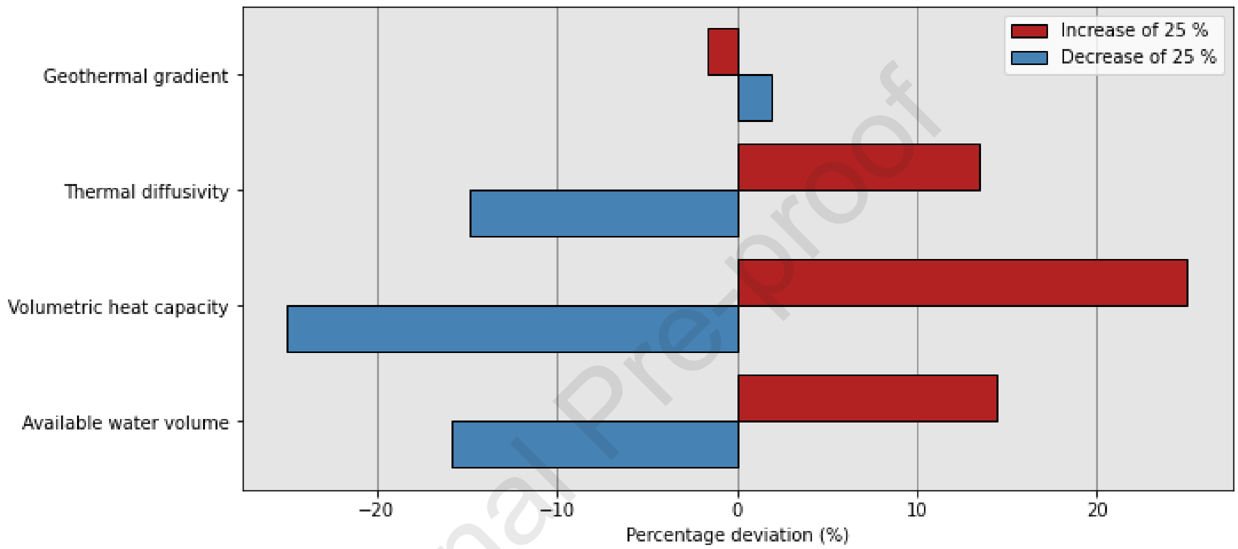

Figure 18. Impact of a ± 25 % variation in initial parameter values on the amount of thermal energy provided by the host rock for a final temperature of 25 °C.

The energy contribution from host rock varies considerably with available water volume. Lower water volume results in a more substantial energy contribution from the rock. For example, the Carey Canadian and King-Beaver mines, with a difference of approximately 8,000,000 m^3 in water volume, exhibit roughly 5 % variance in rock energy contribution (Figure 17). Heat capacity acts as a linear variable that directly influencing energy contribution, increasing proportionally with heat capacity. Likewise, higher thermal diffusivity enables more efficient temperature propagation through the rock, expanding the volume impacted by temperature variations. Consequently, elevated thermal diffusivity amplifies the affected rock volume and boosts the energy contribution. The energy contribution of the rock shows significant variation within temperature differences ranging from 0 to 20 °C. Beyond a temperature difference of 20 °C, the energy contribution plateaus, indicating a less than 2 % difference between final temperatures of 25 and 40 °C (Figure 17).

Assessing the thermal power balance using the volume method is a widely adopted approach recommended by the United States Geological Survey (USGS) for rapid assessment of geothermal resources in water bodies [16,19,59,60]. Wang et al. [61] assessed the low-temperature geothermal resource potential in Chinese provincial capitals using the water volume method, considering energy from surface water sources. The geothermal potential of surface water in this study was assessed considering the energy provided by the volume of water available in lakes and the flow rates for the river resources. The thermal energy contribution of host rocks and water supply was not considered in this study. Similarly, Gaudard et al. [32] explored the potential for using Switzerland's main lakes and rivers as a source of renewable energy for heating and cooling buildings focusing on thermal resources available in water volumes. In these previous studies, the thermal power balance of surface water reservoirs was generally limited to the total thermal energy contained in the water volume alone. In contrast, Bao et al. [17] proposed the estimation of the thermal power balance of the underground galleries in the former Quincy copper mine (USA), considering energy recharge from groundwater flow and host rock with the volume method. This approach was subsequently applied to assess the geothermal resource of the former underground Jiahe coal mine in China [19]. Further use of a thermal power balance approach was made by Ngoyo Mandemvo et al. [31] to evaluate the geothermal potential of the flooded underground Con Mine in the Northwest Territories, Canada. Their study also considered the energy recharge from the groundwater and host rock. The present study builds on the approach by estimating the energetic contribution of water supply and host rock in the thermal balance calculation, but was specifically made for pit lakes, enhancing the methodology for geothermal resource assessment. Previous uses of a thermal power balance were exclusively made for underground mines and needed to be adapted for open-pit mines, for example to calculate the contribution of the host rock since the system geometry is different. The application of this method to the Carey Canadian and King-Beaver mines showed the vast cooling potential of open-pit mines, which contrast to underground mines that are commonly associated with a heating potential.

The analytical approach is a simple and rapid method for conservatively estimating the geothermal resource in a open-pit lake. For example, it does not take into account thermal interactions between different heat transfer mechanisms, nor natural or forced convection phenomena. By focusing solely on conduction, this method makes it possible to estimate temperature propagation through the surrounding rock. However, convection phenomena could recharge the host rock with thermal energy more quickly. Similarly, it should be noted that convection in the water of the pit lake is a phenomenon that recharges thermal energy considerably, but is not taken into account in this simplified analytical approach. Furthermore, this method does not take into account several other natural heat transfer mechanisms that can energetically recharge, to a lesser extent, the available water volume, such as wind, solar radiation, evaporation and terrestrial heat flux.

7. CONCLUSIONS

There is growing interest in harnessing low-temperature geothermal resources from abandoned and flooded mine sites. While numerous studies have assessed the geothermal potential of underground mines, few have focused on open-pit mines. However, many abandoned and flooded mining pits, often located near urban areas, could serve as significant reservoirs of low-temperature geothermal energy.

This work introduces a new analytical approach to estimate the available geothermal resource by evaluating the thermal power balance of the Carey Canadian and King-Beaver pit lakes (Quebec, Canada) using the volume method and an improved thermal power balance calculation. Unlike most studies, this approach goes beyond assessing the thermal resource contained in the volume of water available, offering a comprehensive estimate that considers the energy contribution of host rock and watershed supply. Indeed, over a 25-year exploitation, it has been showed that the host rock can contribute more than 15% of the thermal energy stored in the water body, while the water supply has the potential to double that thermal energy.

However, a major limitation of this analytical approach is its inability to consider possible interactions between pumping and injection points resulting from inadequate geothermal system configuration. Therefore, while the analytical approach can provide a general first-order assessment of the resource, validating a project's feasibility and viability must rely on a more detailed numerical simulation of the system operation.

Developing sustainable geothermal energy sources at mine sites requires a multidisciplinary approach and ongoing collaboration between the scientific community and industry. Despite progress in developing new approaches, technical barriers remain to implementing these unconventional geothermal systems. Providing baseline data and developing accurate methods for resource estimate are essential to overcome these challenges and reducing perception of risk and economic uncertainty among stakeholders interested in such resource development.

8. APPENDIX

8.1 Hydrogeological Balance

8.1.1 Watershed Boundaries

A watershed is a geographical region area that supplies water to a river or a body of water. It is typically defined by watershed lines, identified by ridges and contour lines [49]. In an urban area, boundaries might change due to sewer systems or drainage ditches redirecting surface water, and roads are also often considered as watershed boundaries. Geographic information software was used to delineate the Carey Canadian mine (Figure A.1) and the King-Beaver mine watersheds (Figure A.2) using DTM and DEM data.

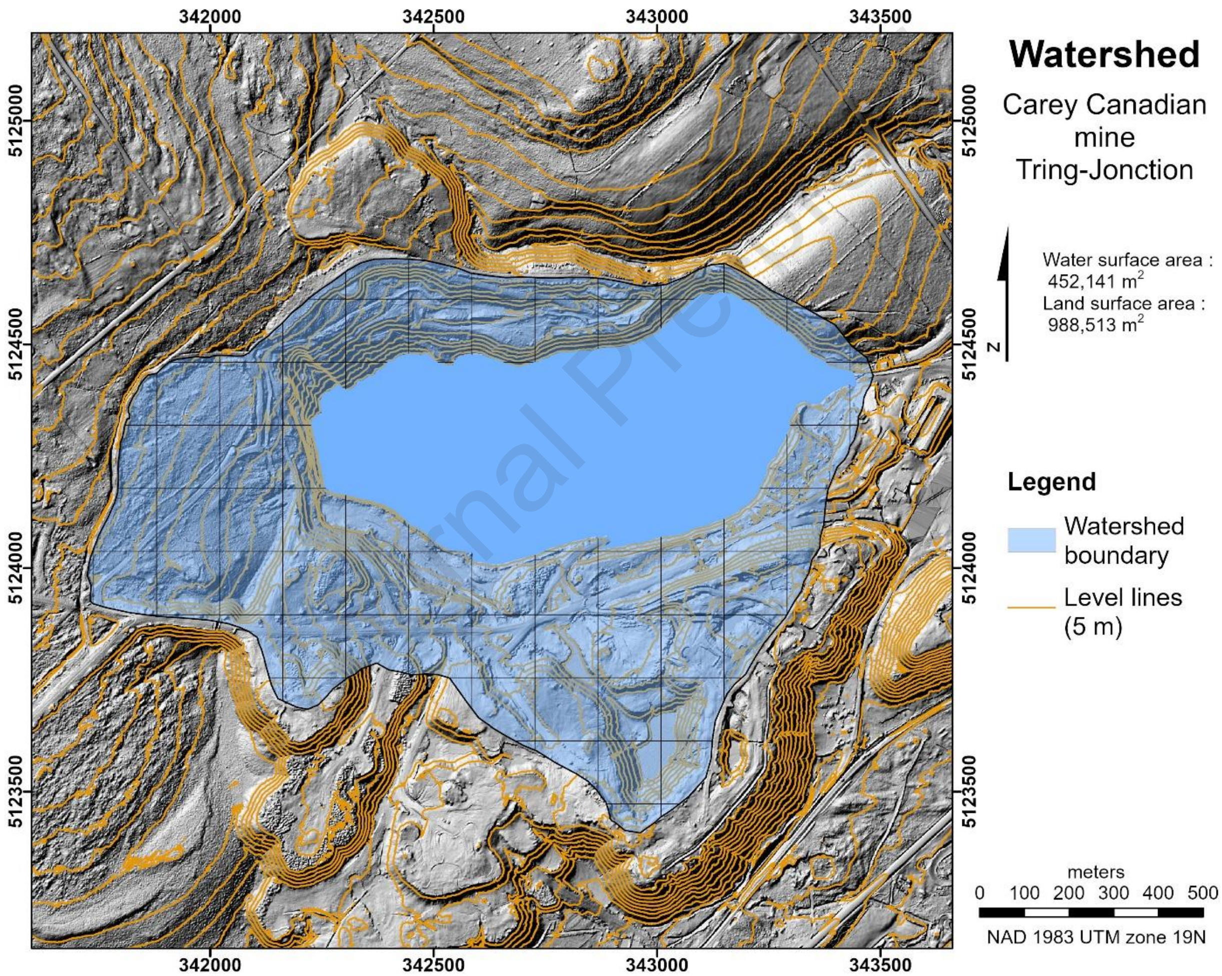

Figure A.1. Carey Canadian mine watershed boundaries and representation of the grid used to estimate the average slope of the regions [35].

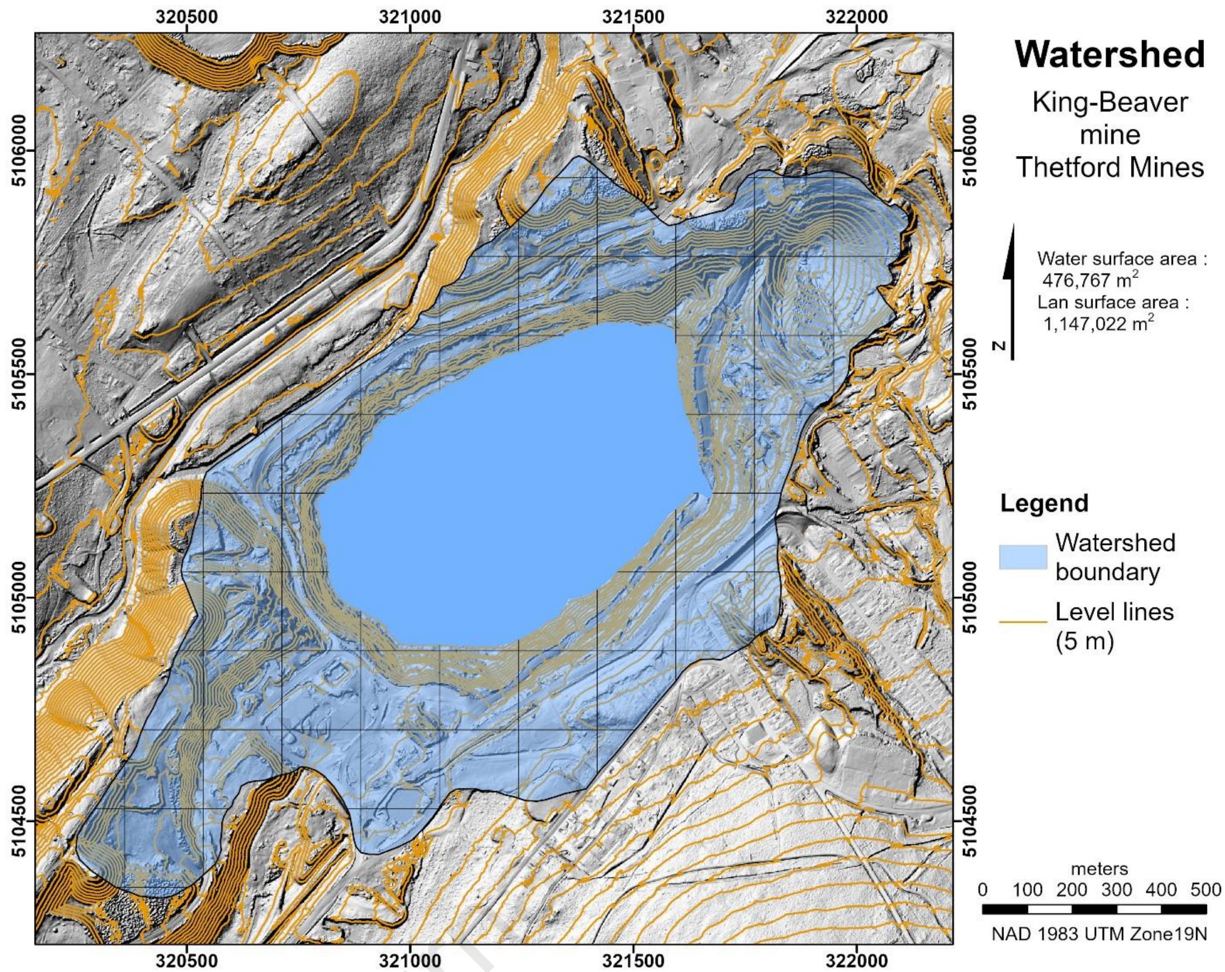

Figure A.2. King-Beaver mine watershed boundaries and representation of the grid used to estimate the average slope of the regions [35].

8.1.2 Infiltration Capacity and Runoff Coefficient

Surface runoff occurs when the precipitation rate (P; mmyr^{-1}) exceeds the soil's infiltration capacity (I; mmyr^{-1}). For runoff to occur, the soil's infiltration capacity must be exceeded. The infiltration can be calculated using the following equation:

$$I^i = P^i - R^i \qquad [A.1]$$

It is important to note that these calculations are performed monthly, with each month represented by the exponent i. The runoff (R; mmyr^{-1}) for each month is computed using the equation:

$$R^i = C_\text{p} P^i \qquad [A.2]$$

The runoff coefficient (C_p) is a dimensionless parameter ranging from 0 to 1 and is used empirically to estimate the amount of runoff water based on total precipitation [49] (

Table A.**1** Table A.2).

Table A.1. Runoff coefficient values for rural areas [49].

Runoff coefficient (C_p)
Rural area

Vegetation	Slope (S_b)	Hydrological classification					
		A	AB	B	BC	C	CD
Cultivation							
Flat	< 3%	0.22	0.30	0.36	0.41	0.47	0.51
Undulating	3 à 8 %	0.25	0.34	0.43	0.51	0.59	0.67
Mountainous	> 8%	0.32	0.43	0.51	0.61	0.67	0.73
Pasture							
Flat	< 3%	0.08	0.12	0.17	0.25	0.34	0.43
Undulating	3 à 8 %	0.10	0.17	0.25	0.33	0.43	0.51
Mountainous	> 8%	0.20	0.29	0.39	0.47	0.56	0.64
Woodlot							
Flat	< 3%	0.04	0.09	0.15	0.21	0.29	0.37
Undulating	3 à 8 %	0.07	0.12	0.19	0.26	0.34	0.43
Mountainous	> 8%	0.11	0.18	0.26	0.34	0.43	0.51
Lake and swamp	-	0.05					

Table A.2. Runoff coefficient values for urban areas [49].

Runoff coefficient (C_p)
Urban area

Description	Minimum	Maximum
Paving (asphalt or concrete)	0.80	0.95
Median strip	0.20	0.40
Gravel road and shoulder	0.40	0.60
Roof	0.70	0.95
Commercial zone		
- Downtown area	0.70	0.95
- Suburb	0.50	0.70
Residential zone		
- Single-family dwelling	0.30	0.50
- Multiple, detached	0.40	0.60
- Multiple attached	0.60	0.75
- Suburb	0.25	0.40
Apartment building	0.50	0.70
Park and cemetery	0.10	0.25
Playground	0.20	0.35
Railroad	0.20	0.35
Waste ground	0.10	0.30

The choice of runoff coefficients for rural areas relies on the hydrological classification of the watershed and its average slope (S_b; [49]). In regions with rugged terrain, the mean slope is estimated using a grid overlaid on the watershed [49] (Figures A.1 and A.2):

$$S_b = \frac{(N_h + N_v)Int}{(L_h + L_v)} \quad [A.3]$$

Here, $L_{(h,v)}$ and $N_{(h,v)}$ respectively stand for the length of the grid lines and the number of times they intersect the contour lines. Int refers to the contour line interval. The average slope of the Carey Canadian and King-Beaver mines is respectively 14.5 % and 21.0 % (Table A.3).

Table A.3. Average slopes of the Carey Canadian and King-Beaver mine watersheds.

	Carey Canadian				**King-Beaver**			
Number of lines	L_v **(m)**	N_v	L_h **(m)**	N_h	L_v **(m)**	N_v	L_h **(m)**	N_h
1	200	3	867	20	208	10	150	4
2	569	8	112	6	83	3	300	15
3	603	9	488	17	568	17	212	1
4	886	23	27	1	774	27	1,096	26
5	255	12	71	2	222	10	1,253	44
6	206	12	88	1	455	13	323	23
7	174	10	422	14	198	14	367	21
8	187	10	154	5	411	20	277	15
9	150	8	454	15	268	24	159	13
10	81	6	152	5	342	19	238	12
11	61	6	817	20	386	26	282	19
12	88	6	606	15	439	23	360	10
13	79	5	1,416	25	233	16	432	23
14	424	14	176	6	374	18	966	33
15	388	14	675	19	1,047	35	122	2
16	619	25	441	15	527	24	245	4
17	614	14	172	5	129	2		
18	476	10						
19	359	7						
20	321	8						
21	383	13						
Summing	**7,123**	**223**	**7,138**	**191**	**6,664**	**301**	**6,782**	**265**
S_b	14.5 %				21.0 %			

According to the Government of Quebec [49], the Thetford Mines region is classified under the hydrological categories AB and B. Consequently, the runoff coefficients for rural regions align with the average value of these categories for the > 8% slope classification in the

Table A.**1**. Urban areas base their runoff coefficients on the average between the minimum and maximum values provided in the Table A.2.
Using the land use types outlined in

Table A.**1**Table A.2, Figure A.5Figure A.4 display the delineation of various sub-areas. These illustrations are used to calculate the weighted average of the watershed runoff coefficient.

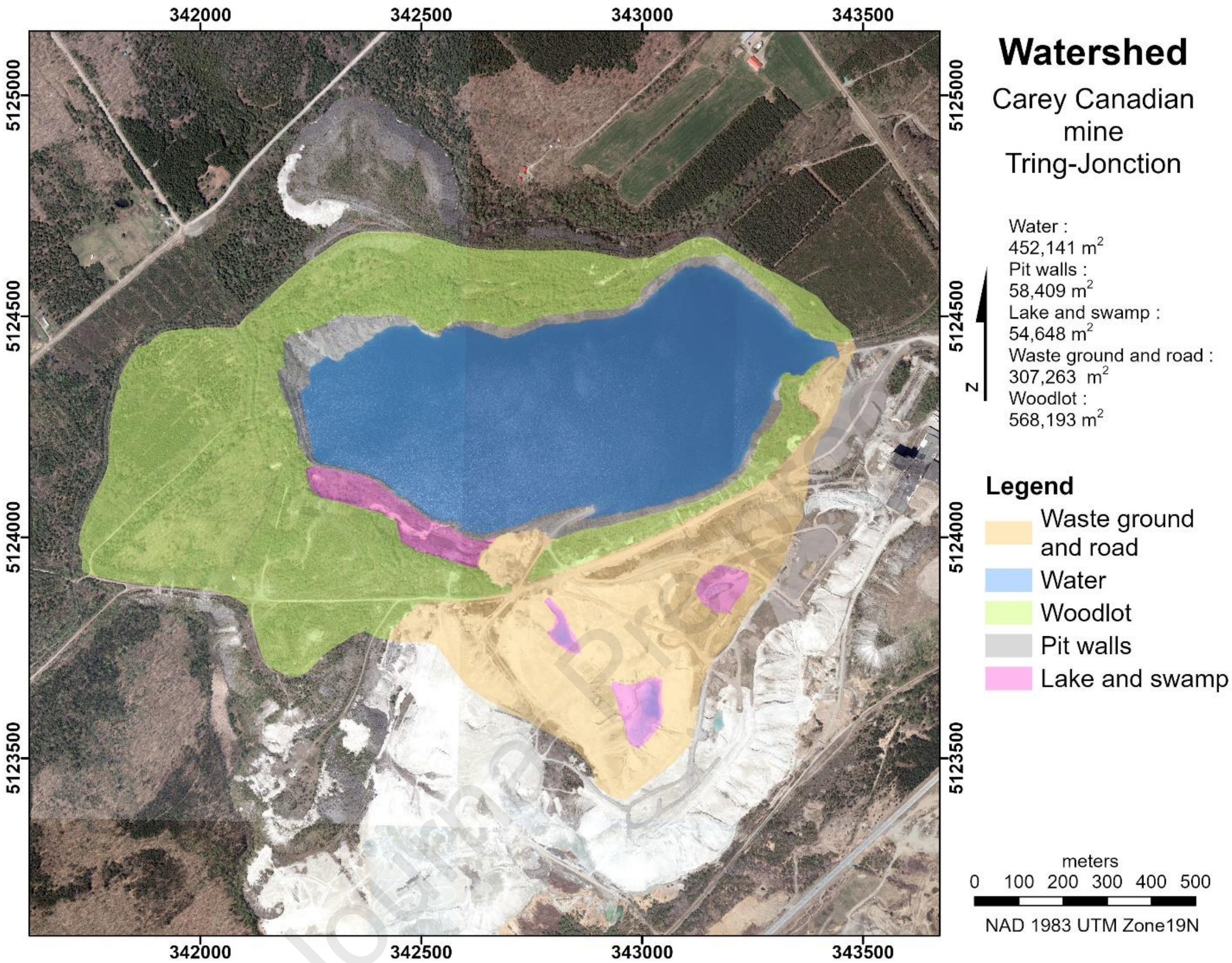

Figure A.3. Discretizations of the Carey Canadian mine watersheds into sub-areas by land use.

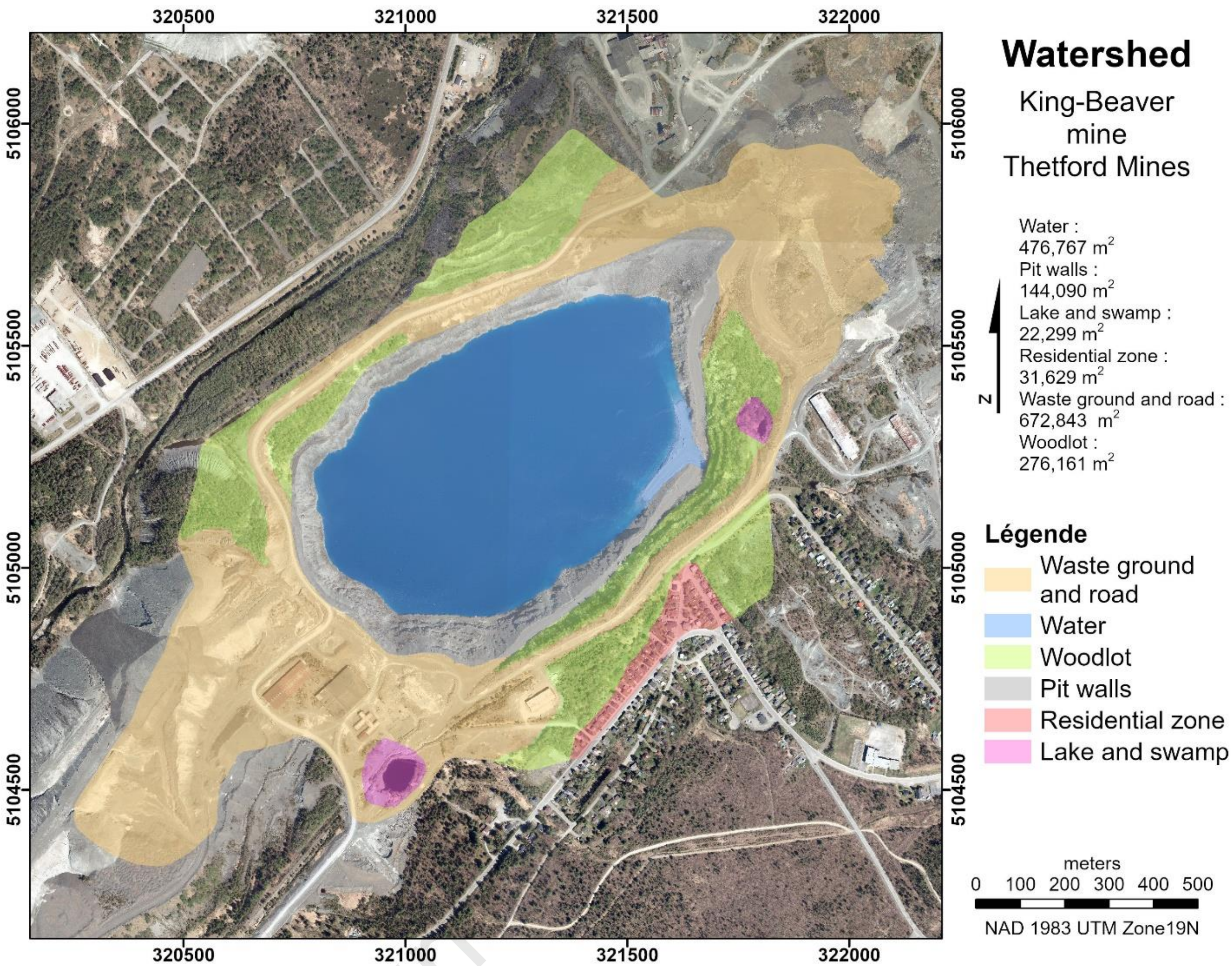

Figure A.4. Discretizations of King-Beaver watersheds into sub-areas by land use.

The overall runoff coefficient for Carey Canadian and King-Beaver mine watersheds, calculated by weighting coefficients assigned to sub-areas, is 0.26 and 0.32 respectively (Table A.4).

Table A.4. Runoff coefficients for the Carey Canadian and King-Beaver mine watersheds.

	Carey Canadian			King-Beaver		
Description	C_p	**Area (m²)**	**Area x C_p**	C_p	**Area (m²)**	**Area x C_p**
Woodlot	0.22	568,193	125,002	0.22	276,161	60,755
Lake and swamp	0.05	54,648	2,732	0.05	22,299	1,115
Pit walls	1.00	58,409	58,409	1.00	144,090	144,090
Gravel road	0.50	28,314	14,157	0.50	69,205	34,603
Waste ground	0.20	278,949	55,790	0.20	603,638	120,728
Suburb				0.33	31,629	10,279
Summing		**988,513**	**256,091**		**1,147,022**	**371,570**
C_p weighted	0.26			0.32		

8.1.3 *Potential and Real Evapotranspiration*

Thornthwaite defines potential evapotranspiration (PET; mmyr^{-1}) as the soil water loss in the absence of any deficit due to vegetation consumption [48,50]:

$$PET^i = 16\left(\frac{10T_{\mathrm{amb}}^i}{I_{\mathrm{t}}}\right)^a F^i \text{ if } T_{\mathrm{amb}}^i > 0\ °C \qquad [A.4]$$

$$PET^i = 0 \text{ if } T_{\mathrm{amb}}^i \leq 0\ °C \qquad [A.5]$$

The variable T_{amb}^i (°C) denotes the average monthly temperature derived from the weather stations within the study regions. I_{t} represents the annual thermal index calculated by summing the monthly thermal indices i^i using the following formula:

$$I_{\mathrm{t}} = \sum_{i=1}^{12} i^i \qquad [A.6]$$

The monthly thermal index can be determined by:

$$i^i = \left(\frac{T_{\mathrm{amb}}^i}{5}\right)^{1.514} \text{ if } T_{\mathrm{amb}}^i > 0\ °C \qquad [A.7]$$

$$i^i = 0 \text{ if } T_{\mathrm{amb}}^i \leq 0\ °C \qquad [A.8]$$

The constant parameter a is assessed through the following equation:

$$a = 6.75x10^{-7}I_{\mathrm{t}}^3 - 7.71x10^{-5}I_{\mathrm{t}}^2 + 1.79x10^{-2}I_{\mathrm{t}} + 0.49239 \qquad [A.9]$$

Lastly, F^i represents the correction coefficient, accounting for the average monthly sunshine duration. This coefficient is defined based on the month and latitude of the study areas [50].

When plants begin to wilt, it signifies that soil moisture has fallen below its capacity to resist the force of gravity at the surface. This state of reduced water availability can restrict real evapotranspiration (RET; mmyr^{-1}) to levels lower than potential evapotranspiration. Consequently, real evapotranspiration relies on both the available water reserves at the soil surface (S; mmyr^{-1}) and the deficit soil moisture (D; mmyr^{-1}; [48,50].

Table A.**5** provides a grid facilitating the calculation of actual evapotranspiration, water reserve, and recharge (G; mmyr^{-1}) based on soil moisture deficit. This table is derived from Thornthwaite's (1948) hydrogeological balance calculation method.

Table A.5. Calculation grid for determining real evapotranspiration, soil water reserves and recharge.

D^i	RET^i	Si	Gi
< 0	$S_{i-1} + I^i$	0	0
= 0	PET^i	0	0
> 0 and < S_{max}	PET^i	D^i	0
> S_{max}	PET^i	S_{max}	D^i - S_{max}

The moisture deficit is determined using the following equation:

$$D^i = S^{i-1} + I^i - PET^i \quad [A.10]$$

To initiate the calculation in January, the initial value of the available water reserve (S^0) is considered as the maximum reserve ($S_{\max}$). In cases where data is unavailable, $S_{\max}$ is approximated as 10 % moisture in the top meter of soil, which equals 100 mm [48,50].

8.1.4 Annual Water Supply

The hydrogeological balance outcomes for the Carey Canadian mine watershed were calculated based on Thornthwaite's approach and are outlined in Table A.6. Similarly,

Table A.**7** contains the hydrogeological balance outcomes for the King-Beaver mine watershed.

Table A.6. Thornthwaite hydrogeological assessment of the Carey Canadian mine watershed.

Month	Mean temp. (°C)	P (mm)	R (mm)	I (mm)	PET (mm)	RET (mm)	G (mm)
January	-12.2	88.9	23.0	65.9	0.0	0.0	65.9
February	-10.3	72.0	18.6	53.4	0.0	0.0	53.4
March	-5.3	74.3	19.2	55.1	0.0	0.0	55.1
April	2.8	78.7	20.4	58.3	18.7	18.7	39.6
May	10.1	101.5	26.3	75.2	70.2	70.2	5.0
June	15.1	130.0	33.7	96.3	102.9	102.9	0.0
July	17.9	136.6	35.4	101.2	122.4	122.4	0.0
August	16.8	128.0	33.2	94.8	106.6	106.6	0.0
September	12.5	111.5	28.9	82.6	69.5	69.5	0.0
October	5.4	118.8	30.8	88.0	28.8	28.8	32.9
November	-0.8	91.7	23.8	67.9	0.0	0.0	67.9
December	-8.3	88.7	23.0	65.7	0.0	0.0	65.7
Annual	**3.6**	**1,220.7**	**316.2**	**904.5**	**519.1**	**519.1**	**385.4**

Table A.7. Thornthwaite hydrogeological assessment of the King-Beaver mine watershed.

Month	Mean temp. (°C)	P (mm)	R (mm)	I (mm)	PET (mm)	RET (mm)	G (mm)
January	-11.60	108.00	34.99	73.01	0.00	0.00	73.01
February	-9.50	86.50	28.03	58.47	0.00	0.00	58.47
March	-4.00	89.00	28.84	60.16	0.00	0.00	60.16
April	3.90	88.80	28.77	60.03	23.52	23.52	36.50
May	11.10	104.90	33.99	70.91	73.87	73.87	0.00
June	16.10	130.00	42.12	87.88	106.97	106.97	0.00
July	18.60	133.30	43.19	90.11	125.04	125.04	0.00
August	17.60	135.30	43.84	91.46	109.43	109.43	0.00
September	13.20	100.10	32.43	67.67	71.06	71.06	0.00
October	6.50	112.20	36.35	75.85	32.20	32.20	0.00
November	0.10	104.60	33.89	70.71	0.00	0.00	36.03
December	-7.40	117.20	37.97	79.23	0.00	0.00	79.23
Annual	**4.60**	**1,309.90**	**424.41**	**885.49**	**542.08**	**542.08**	**343.41**

9. Abacuses for rock energy contribution

To simplify the estimation of the host rock's energy contribution in pit lakes, four abacuses have been created for situations where the temperature difference between the initial and final water temperature is 5, 10, 15 and 20 °C (Figure A.5Figure A.6Figure A.7Figure A.8). The abacuses have been designed for use in any pit lake with an available water volume ranging from 20,000,000 to 80,000,000 m^3. They estimate the host rock's energy contribution as a function of the energy contained in the water volume utilizing a range of feasible thermal rock properties determined from literature reviews [39,40,42,43]. Assumptions include an initial water temperature of 4 °C, a 25-year operational span, and a geothermal gradient of 0.03 $°Cm^{-1}$. These abacuses allow a quick and practical estimation of the energy contribution of the host rock, avoiding tedious calculations and providing approximate values for different temperature configurations. However, it is important to note that these estimates are based on simplifying assumptions, and that detailed analyses may require more advanced approaches. An example of how to use the abacus can be found in the appendix, showing the evaluation of the host rock's energy contribution at the Carey Canadian and King-Beaver mines.

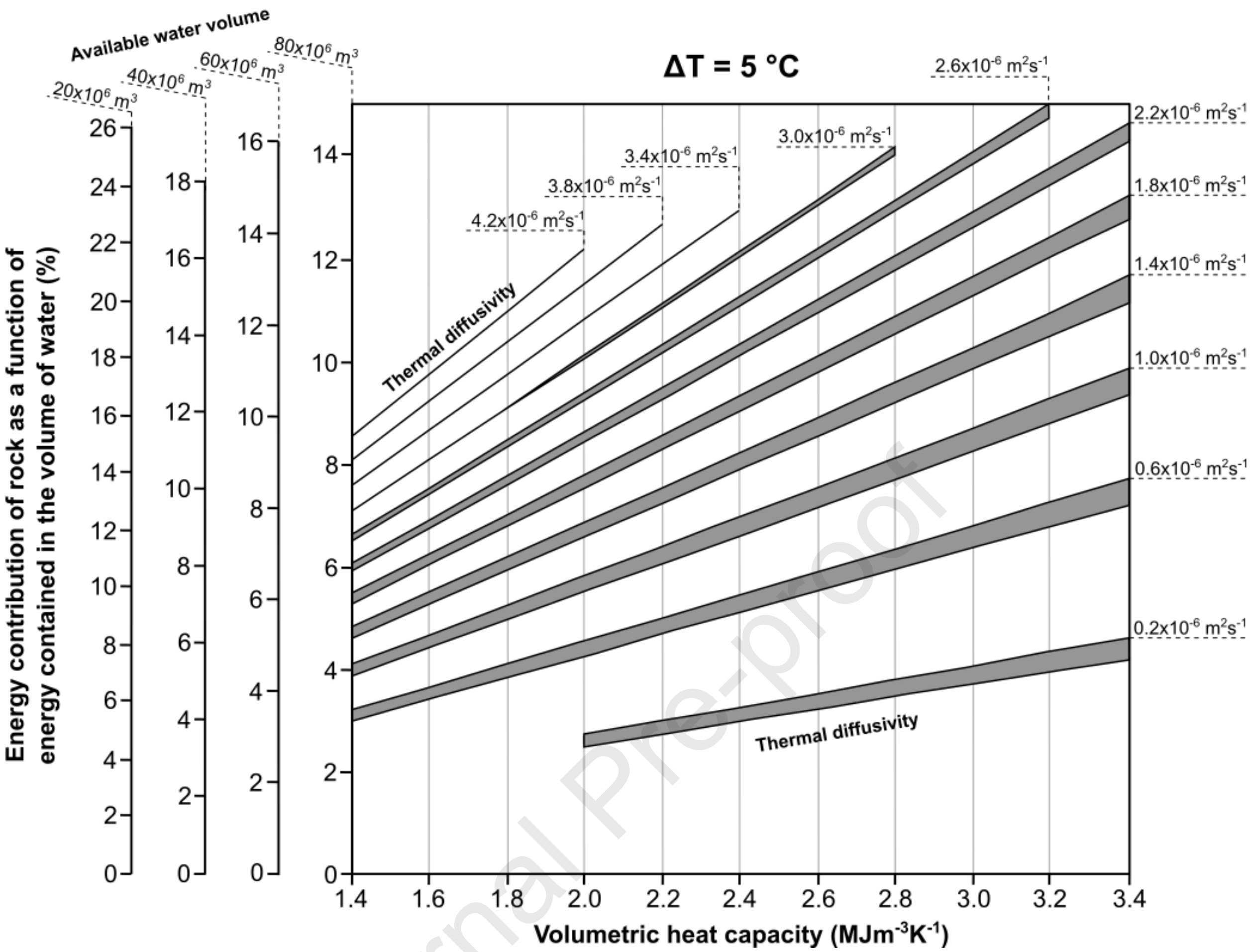

Figure A.5. Abacus for estimating the energy contribution of the host rock according to the energy contained in different volumes of water and different values of thermal properties for a temperature difference of 5 °C between the initial temperature of the water and its final temperature after exploitation.

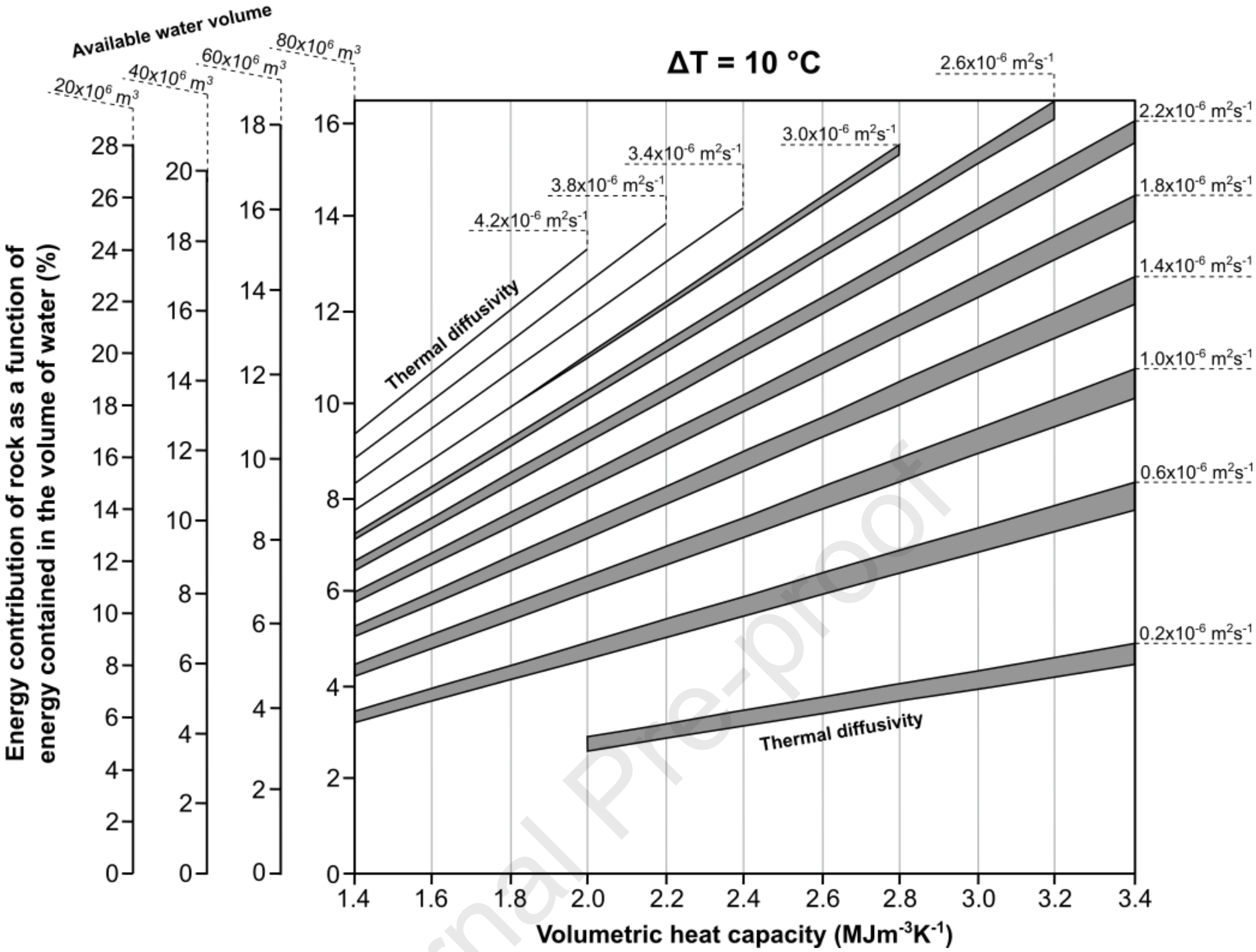

Figure A.6. Abacus for estimating the energy contribution of the host rock according to the energy contained in different volumes of water and different values of thermal properties for a temperature difference of 10 °C between the initial temperature of the water and its final temperature after exploitation.

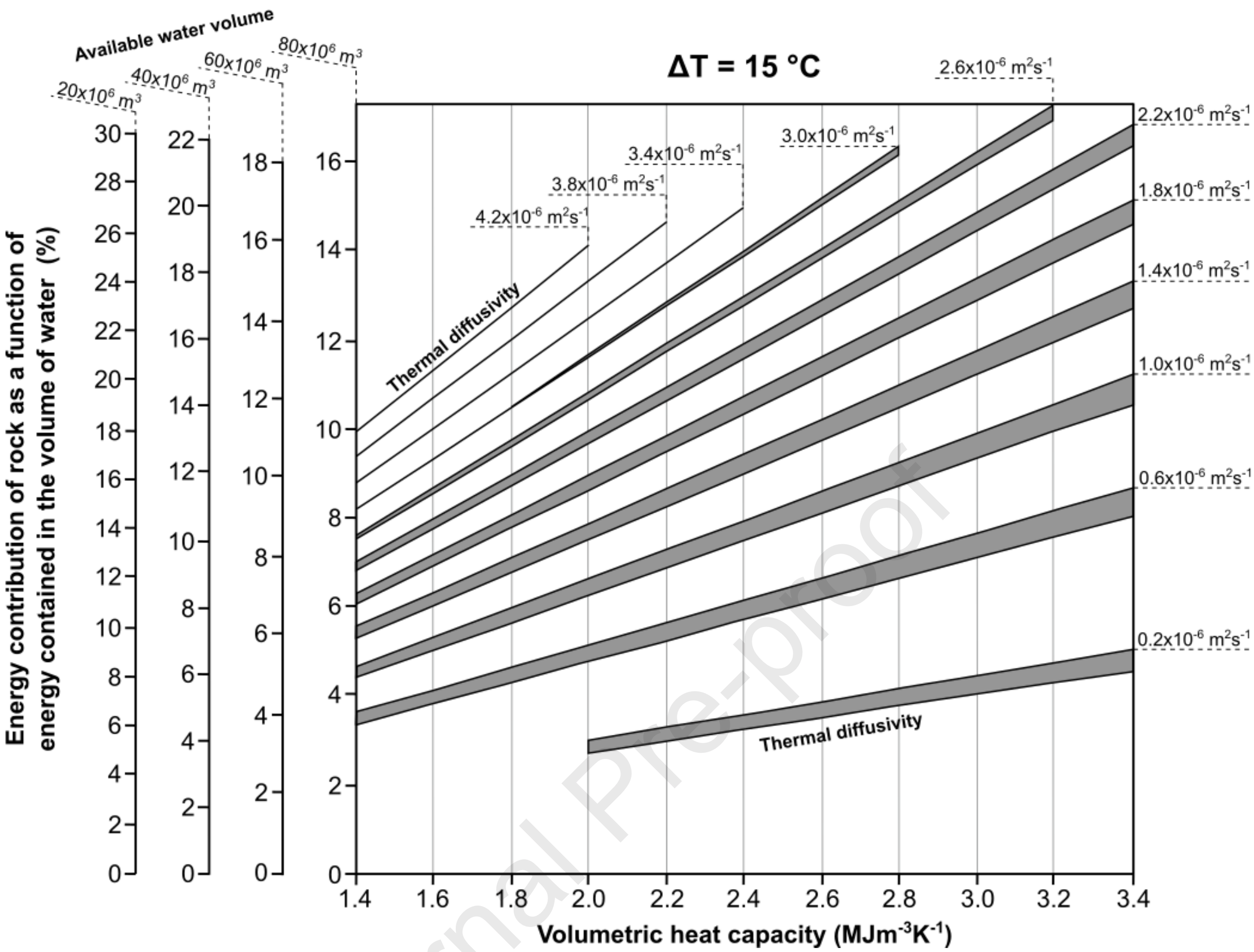

Figure A.7. Abacus for estimating the energy contribution of the host rock according to the energy contained in different volumes of water and different values of thermal properties for a temperature difference of 15 °C between the initial temperature of the water and its final temperature after exploitation.

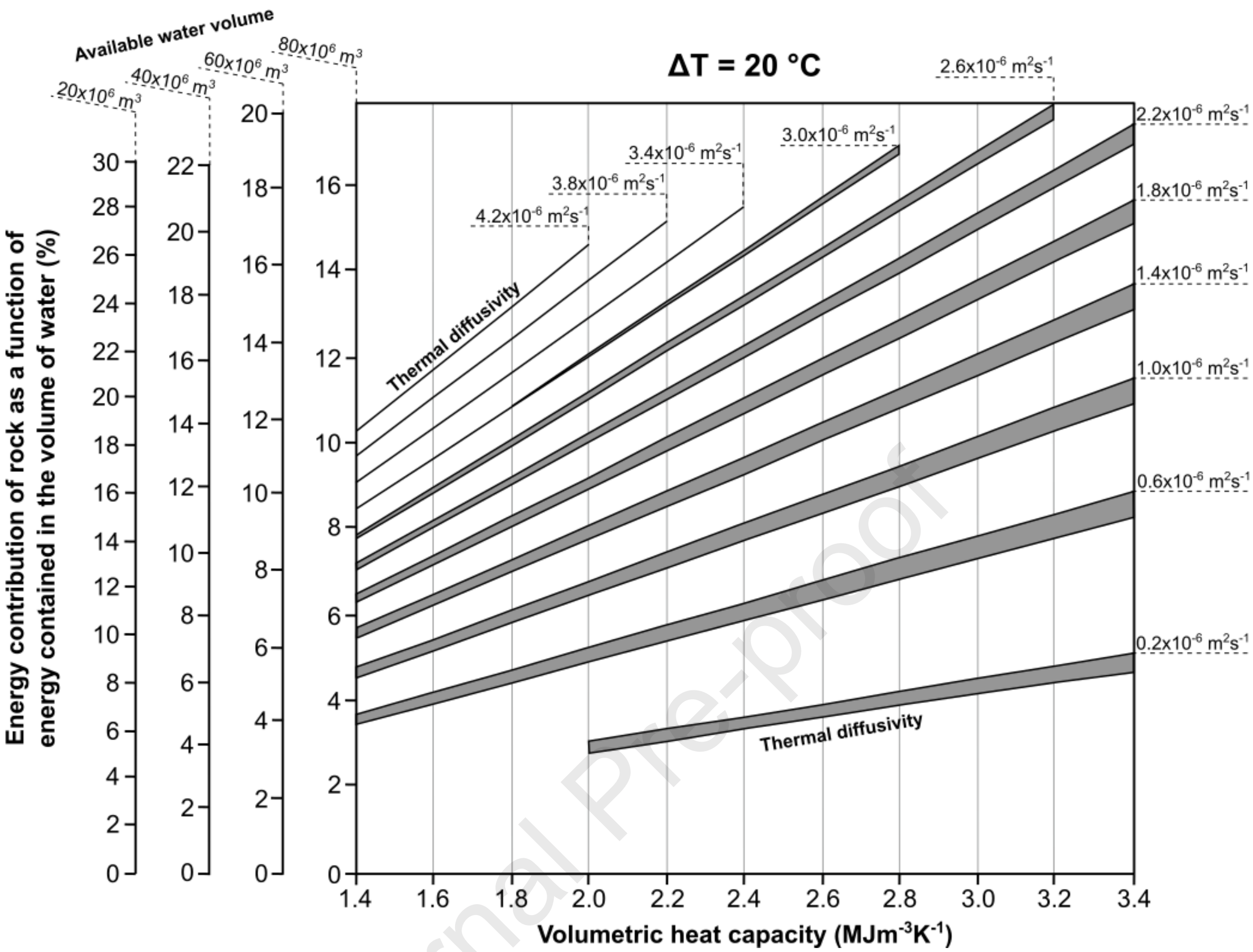

Figure A.8. Abacus for estimating the energy contribution of the host rock according to the energy contained in different volumes of water and different values of thermal properties for a temperature difference of 20 °C between the initial temperature of the water and its final temperature after exploitation.

Figure A.9 represents two instances illustrating the abacus application, employing the Carey Canadian and King-Beaver mines for a temperature variance of 20°C.

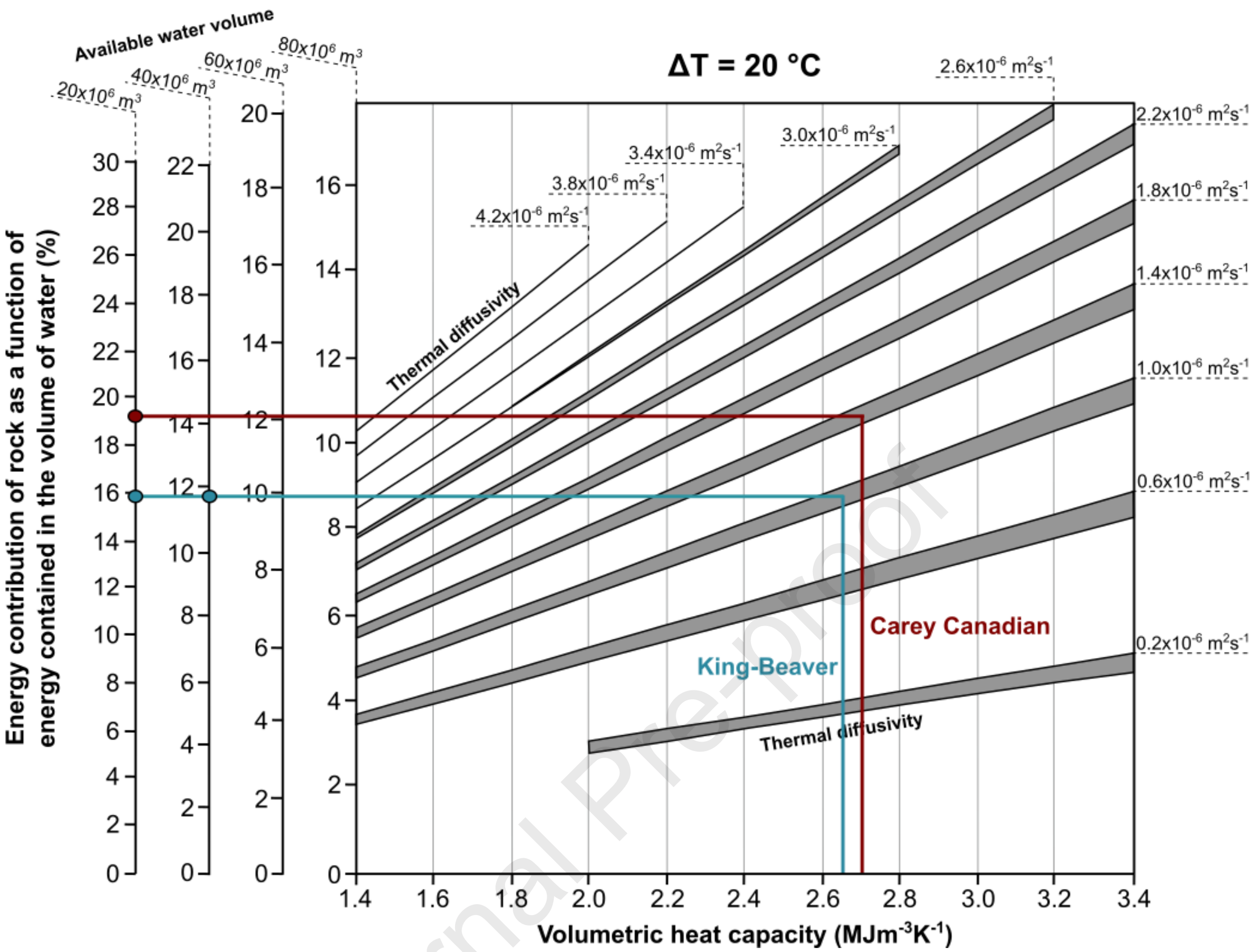

Figure A.9. Examples of the estimated of host rock's energy contribution based on the thermal energy available in the water volume for Carey Canadian and King-Beaver.

In the case of the Carey Canadian mine, considering a volumetric heat capacity of 2.73 $MJm^{-3}K^{-1}$, a thermal diffusivity of 1.39 mm^2s^{-1}, and an available water volume of approximately 20,000,000 m^3, the rock's energy contribution, assessed with the abacus, aligns with about 19 % of the energy within the pit's water volume. This result closely resembles the initial estimate in Figure 17, where the rock contributed to around 18.8 % of the water volume's energy. For the King-Beaver mine, the volumetric heat capacity and thermal diffusivity were estimated at 2.65 $MJm^{-3}K^{-1}$ and 1.04 mm^2s^{-1} respectively, and the water volume ranges between 20,000,000 and 40,000,000 m^3 along the vertical axes. This allows the estimation of the rock's energy contribution by averaging the values corresponding to these two axes:

$$\frac{15.9\,\% + 11.8\,\%}{2} = \frac{27.7\,\%}{2} = 13.9\,\% \qquad [A.11]$$

The abacus indicates that the energy contribution from the host rock amounts to approximately 13.9 % of the energy contained in the water volume, closely aligning with the initial calculation of 13.8 %.

10. REFERENCES

[1] Tajvidi Asr, E., Kakaie, R., Ataei, M., Tavakoli Mohammadi, M. R., 2019. A review of studies on sustainable development in mining life cycle. Journal of Cleaner Production 229: 213-231. https://doi.org/10.1016/j.jclepro.2019.05.029
[2] Laurence, D., 2006. Optimisation of the Mine Closure Process. Journal of Cleaner Production 14 (3–4): 285–98. https://doi.org/10.1016/j.jclepro.2004.04.011
[3] Peralta Ramos, E., Breede, K., Falcone, G., 2015. Geothermal Heat Recovery from Abandoned Mines: A Systematic Review of Projects Implemented Worldwide and a Methodology for Screening New Projects. Environmental Earth Sciences. 73(11).6783–95. https://doi.org/10.1007/s12665-015-4285-y
[4] Loredo, C., Roqueñí, N., Ordóñez, A., 2016. Modelling Flow and Heat Transfer in Flooded Mines for Geothermal Energy Use: A Review. International Journal of Coal Geology. 164.115–22. https://doi.org/10.1016/j.coal.2016.04.013
[5] Al-Habaibeha, A., Athresha, A.P., Parker, K., 2018. Performance analysis of using mine water from an abandoned coal mine for heating of buildings using an open loop based single shaft GSHP system. Applied Energy 21(1): 393-402. https://doi.org/10.1016/j.apenergy.2017.11.025
[6] Sarbu, I., Sebarchievici, C., 2014. General Review of Ground-Source Heat Pump Systems for Heating and Cooling of Buildings. Energy and Buildings. http://dx.doi.org/10.1016/j.enbuild.2013.11.068
[7] Raymond, J., Therrien, R., Gosselin, L., 2010. Low-Temperature Geothermal Energy in Mining Environments. CIM Journal. 1(2).11.
[8] Omer, A.M. 2008. Ground-Source Heat Pumps Systems and Applications. Renewable and Sustainable Energy Reviews. https://doi.org/10.1016/j.rser.2006.10.003
[9] Comeau, F.-A., Raymond. J., 2018. Revue de la littérature sur les règlements et les normes relatifs aux systèmes de pompes à chaleur géothermique face à la protection des prélèvements d'eau. Institut national de la recherche scientifique - Centre Eau Terre Environnement. Quebec. https://www.environnement.gouv.qc.ca/eau/prelevements/reglement-prelevement-protection/evaluation-normes/juin2018/Revue-RPEP-ChapIV-syst-geothermiques.pdf
[10] Lund, J.W., Huttrer, G.W., Toth, A.N., 2022 Characteristics and trends in geothermal development and use, 1995 to 2020. Geothermics 105, 102522, https://doi.org/10.1016/j.geothermics.2022.102522
[11] Grasby, S. E., Allen, D. M., Bell, S., Chen, Z., Ferguson, G., Jessop, A., Kelman, M., Ko, M., Majorowicz, J., Moore, M., Raymond, J., Therrien, R., 2012. Geothermal Energy Resource Potential of Canada. Public report. 6914. https://doi.org/10.4095/291488
[12] Raymond, J., Therrien, R., 2014. Optimizing the design of a geothermal district heating and cooling system located at a flooded mine in Canada. Hydrogeology 22: 217–231. https://doi.org/10.1007/s10040-013-1063-3
[13] Jessop, A.M., Macdonald, J.K., Spence, H., 1995. Clean Energy from Abandoned Mines at Springhill, Nova Scotia. Energy Sources. 17(1).93–106. https://doi.org/10.1080/00908319508946072
[14] Raymond, J., Therrien, R., 2008. Low-Temperature Geothermal Potential of the Flooded Gaspé Mines, Québec, Canada. Geothermics. 37(2).189–210. https://doi.org/10.1016/j.geothermics.2007.10.001
[15] Hall, A., Scott, J. A., Shang, H., 2011. Geothermal Energy Recovery from Underground Mines. Renewable and Sustainable Energy Reviews. 15(2).916–24. https://doi.org/10.1016/j.rser.2010.11.007

[16] Preene, M., Younger, P. L., 2014. Can You Take the Heat? – Geothermal Energy in Mining. Mining Technology. 123(2).107–18. https://doi.org/10.1179/1743286314Y.0000000058
[17] Bao, T., Meldrum, J., Green, C., Vitton, S., Liu, Z., Bird. K., 2019. Geothermal Energy Recovery from Deep Flooded Copper Mines for Heating. Energy Conversion and Management 183(3): 604–16. https://doi.org/10.1016/j.enconman.2019.01.007
[18] Banks, D., Athresh, A. Al-Habaibeh, A., Burnside. N., 2019. Water from Abandoned Mines as a Heat Source: Practical Experiences of Open- and Closed-Loop Strategies, United Kingdom. Sustainable Water Resources Management 5(1): 29–50. https://doi.org/10.1007/s40899-017-0094-7
[19] Chu, Z., Dong, K., Gao, P. Wang, Y., Sun. Q., 2021. Mine-Oriented Low-Enthalpy Geothermal Exploitation: A Review from Spatio-Temporal Perspective. Energy Conversion and Management 237(June): 114123. https://doi.org/10.1016/j.enconman.2021.114123
[20] Banks, D., Steven, J., Black, A., Naismith. J., 2022. Conceptual Modelling of Two Large-Scale Mine Water Geothermal Energy Schemes: Felling, Gateshead, UK. International Journal of Environmental Research and Public Health 19(3): 1643. https://doi.org/10.3390/ijerph19031643
[21] Ngoyo Mandemvo, D.D., Comeau, F.-A., Raymond, J., Grasby, S.E., Terlaky, V., 2024. Numerical Assessment of the Geothermal and Thermal Energy Storage Potential of the Underground Con Mine (Northwest Territories, Canada). Mine Water and the Environment. https://doi.org/10.1007/s10230-024-00976-4
[22] Kavanaugh, S.P. and Rafferty, K., 1997. Design of Geothermal Systems for Commercial and Institutional Buildings. American Society of Heating, Refrigeration and Air-Conditioning Engineers (ASHRAE), 167 pp.
[23] Banks, D., 2012. Pond- and Lake-Based Ground Source Heat Systems. In Chapter 12 - An Introduction to Thermogeology: Ground Source Heating and Cooling. John Wiley & Sons, Ltd. 353-371. https://doi.org/10.1002/9781118447512.ch12
[24] Hostetler, S.W., 1995. Hydrological and thermal response of lakes to climate: Description and modeling. In: Lerman, A., Imboden, D.M. and Gat, J.R. (eds.), Physics and Chemistry of Lakes, 2nd Edition. Springer-Verlag, Berlin, 63–82.
[25] Rouse, W.R., Oswald, C.J., Binyamin, J., Spence, C., Schertzer, W.M., Blanken, P.D., Bussières, N., Duguay, C.R., 2005. The role of northern lakes in a regional energy balance. Journal of Hydrometeorology 6: 291–305. https://doi.org/10.1175/JHM421.1

[26] Chicco, J. M., Comeau, F.-A., Casasso, A., Comina, C., Giordano, N., Mandrone, G., Raymond. J., 2021. Alternative Use of Artificial Quarry Lakes as a Source of Thermal Energy for Greenhouses. Water 13(24): 3560. https://doi.org/10.3390/w13243560
[27] Barral, N., Husillos, R., Castillo, E., Cánovas, M., Lam, E. J., Calvo. L., 2021. Volumetric Quantification and Quality of Water Stored in a Mining Lake: A Case Study at Reocín Mine (Spain). Minerals 11(March): 212. https://doi.org/10.3390/min11020212
[28] Raymond, J., Therrien, R., Hassani, F., 2008. Overview of Geothermal Energy Resources in Québec (Canada) Mining Enviroments. Proceeding of the 10th International Mine Water Association Congress. Karlovy Vary, 12.
[29] Henderson-Sellers, B., 1986. Calculating the Surface Energy Balance for Lake and Reservoir Modeling: A Review. Reviews of Geophysics. 24(3).625–49. https://doi.org/10.1029/RG024i003p00625
[30] Schmid, M., Read, J., 2022. Heat Budget of Lakes. Dans Encyclopedia of Inland Waters. Elsevier. 467–73. https://doi.org/10.1016/B978-0-12-819166-8.00011-6

[31] Ngoyo Mandemvo, D.D., Comeau, F.-A., Raymond, J., Grasby, S.E., Terlaky, V., 2023. Geothermal Potential of Closed Underground Mines: Resource Assessment Study of the Con Mine, Northwest Territories, Canada. Natural Resources Research. 32(4)1579–93. https://doi.org/10.1007/s11053-023-10214-3
[32] Gaudard, A., Wüest, A., Schmid. M., 2019. Using Lakes and Rivers for Extraction and Disposal of Heat: Estimate of Regional Potentials. Renewable Energy 134(April): 330–42. https://doi.org/10.1016/j.renene.2018.10.095
[33] Hébert, Y., 1985. Géologie des gîtes et indices de talc de la région de Thetford Mines. Public report. MB 85-38. Ministère de l'Énergie et des Ressources Naturelles. Quebec.
[34] Slivitzky, A., St-Julien, P., 1987. Compilation géologique de la région de l'Estrie-Beauce. Public report. MM 85-04. Ministère de l'Énergie et des Ressources Naturelles. Quebec.
[35] Government of Canada, 2021. GeoGratis. Website. Consulted in 2021. https://geogratis.gc.ca/
[36] MERN, (Ministère de l'Énergie et des Ressources Naturelles), 2021. SIGÉOM - Système d'information Géominière. Website. Consulted in 2021. https://sigeom.mines.gouv.qc.ca/signet/classes/I1102_indexAccueil?l=f
[37] Riordon, P.H., 1975. Géologie des gîtes d'amiante du sud-est québécois. Public report. ES 018. Ministère de l'Énergie et des Ressources Naturelles. Quebec.
[38] Popov, Y., Beardsmore, G., Clauser, C., Roy, S., 2016. ISRM Suggested Methods for Determining Thermal Properties of Rocks from Laboratory Tests at Atmospheric Pressure. Rock Mechanics and Rock Engineering. 49(10).4179–4207.
https://doi.org/10.1007/s00603-016-1070-5
[39] Clauser, C., Huenges. E., 1995. Thermal Conductivity of Rocks and Minerals. In Rock Physic and Phase Relations, 23. United States of America. American Geophysical Union.
[40] Waples, D.W., Waples, J. S., 2004. A Review and Evaluation of Specific Heat Capacities of Rocks, Minerals, and Subsurface Fluids. Part 1: Minerals and Nonporous Rocks. Natural Resources Research. 13(2).97–122. https://doi.org/10.1023/B:NARR.0000032647.41046.e7
[41] Schön, J., 2011. Physical Properties of Rocks: A Workbook. Handbook of Petroleum Exploration and Production 8. Elsevier. Boston
[42] Eppelbaum, L., Kutasov, I., Pilchin. A., 2014. Applied Geothermics. Lecture Notes in Earth System Sciences. Berlin, Heidelberg. Springer Berlin Heidelberg. https://doi.org/10.1007/978-3-642-34023-9
[43] Dalla Santa, G., Galgaro, A., Sassi, R., Cultrera, M., Scotton, P., Mueller, J., Bertermann, D., Mendrinos, D., Pasquali, R., Perego, R., Pera, S., Di Sipio, E., Cassiani, G., De Carli, M., Bernardi, A., 2020. An Updated Ground Thermal Properties Database for GSHP Applications. Geothermics 85: 101758. https://doi.org/10.1016/j.geothermics.2019.101758
[44] Misener, A.D., Thompson, L. G.D., 1950. Temperature Gradients in Ontario and Quebec. The Canadian Mining and Metallurgical Trans. LIII.380–83.
[45] Ouzzane, M., Eslami-Nejad, P., Badache, M., Aidoun, Z. 2015. New Correlations for the Prediction of the Undisturbed Ground Temperature. Geothermics. 53.379–84. https://doi.org/10.1016/j.geothermics.2014.08.001
[46] Government of Canada, 2011. Normales climatiques canadiennes - Climat - Environnement et Changement climatique Canada. Website. Consulted in 2021. https://climat.meteo.gc.ca/climate_normals/index_f.html
[47] Welch, P.S., 1948. Limnological Methods. McGraw-Hill Book Company Inc. United States of America.

[48] Thornthwaite, C.W., 1948. An Approach toward a Rational Classification of Climate. Geographical Review. 38(1).55. https://doi.org/10.2307/210739
[49] Government of Quebec, 2014. Manuel de conception des ponceaux. Bibliothèque et Archives nationales du Québec. ISBN: 978-2-551-25589-4 http://www3.publicationsduquebec.gouv.qc.ca/produits/ouvrage_routier.fr.html
[50] Pédelaborde, P., 2005. Les bilans hydriques. Cahiers de géographie du Québec. 12(25).5–23. https://doi.org/10.7202/020784ar
[51] Gammons, C. H., Harris, L. N., Castro, J. M., Cott, P. A., Hanna. B. W., 2009. Creating Lakes from Open Pit Mines: Processes and Considerations - with Emphasis on Northern Environments. Canadian Technical Report of Fisheries and Aquatic Sciences 2826, 106 p.
[52] Chiasson, A.D., 1999. Advances in Modeling of Ground-Source Heat Pump Systems. Master thesis, Ontario, Canada, University of Windsor.
[53] RAPPEL, (Experts-conseils en environnement et en gestion de l'eau), 2021. Composantes d'un lac. Webside. Consulted in 2021. https://rappel.qc.ca/fiches-informatives/composantes-dun-lac/
[54] Muffler, P., Cataldi, R., 1977. Methods for Regional Assessment of Geothermal Resources. Public report. 77–870. Geological Survey. United States of America.
[55] Incropera, F. P., DeWitt, D. P., Bergman, T. L., Lavine, A. S., 2007. Fundamentals of Heat and Mass Transfer. 6e Édition. John Wiley & Sons, Inc. United States of America. ISBN : 0-471-45728-0
[56] Cengel, Y.A., et Boles., M.A., 2006. Thermodynamics: An Engineering Approach. 5e ed. McGraw-Hill.
[57] Comeau, F.-A., Raymond, J., Ngoyo Mandemvo. D.D., 2019. Évaluation du potentiel géothermique des mines désaffectées de Société Asbestos limitée à Thetford Mines. Research report. Institut national de la recherche scientifique - Centre Eau Terre Environnement. Quebec
[58] Ngoyo Mandemvo, D.D., 2019. Potentiel géothermique des mines abandonnées de Société Asbestos Limitée (SAL) à Thetford Mines au Québec, Canada : cas de la mine King Beaver. Master thesis, University of Mons. Belgium.
[59] Walsh, W., 2013. Geothermal Resource Assessment of the Clarke Lake Gas Field, Fort Nelson, British Columbia. Bulletin of Canadian Petroleum Geology. 61(3).241–51. https://doi.org/10.2113/gscpgbull.61.3.241
[60] Chudy, K., 2022. Mine Water as Geothermal Resource in Nowa Ruda Region (SW Poland). Water 14 (2): 136. https://doi.org/10.3390/w14020136
[61] Wang, G., Wang, W., Luo, J., Zhang, Y., 2019. Assessment of Three Types of Shallow Geothermal Resources and Ground-Source Heat-Pump Applications in Provincial Capitals in the Yangtze River Basin, China. Renewable and Sustainable Energy Reviews. 111.392–421. https://doi.org/10.1016/j.rser.2019.05.029

Declaration of interests

☐ The authors declare that they have no known competing financial interests or personal relationships that could have appeared to influence the work reported in this paper.

☒ The authors declare the following financial interests/personal relationships which may be considered as potential competing interests:

Jasmin Raymond reports financial support was provided by Quebec Research Fund Nature and Technology. If there are other authors, they declare that they have no known competing financial interests or personal relationships that could have appeared to influence the work reported in this paper.